AD-A104 169 H S S INC BEDFORD MA F/G 4/1
REMOTE SENSING OF ATMOSPHERIC VISIBILITY: A CRITICAL REVIEW.(U)
APR 78 H P SMULER, H S STEWART F19628-77-C-0202
UNCLASSIFIED HSS-8-041 AFGL-TR-78-0216 NL

END
DATE FILMED
10-81
DTIC

AFGL-TR-78-0216

REMOTE SENSING OF ATMOSPHERIC VISIBILITY: A CRITICAL REVIEW

Marion P. Shuler, Jr.

Harold S. Stewart

HSS Inc
2 Alfred Circle
Bedford, Mass 01730

30 April 1978

Final Report for Period 8 Jul 1977 to 30 Apr 1978

Approved for public release; distribution unlimited.

This research was supported by the Air Force In-House Laboratory Independent Research Fund.

AIR FORCE GEOPHYSICS LABORATORY
AIR FORCE SYSTEMS COMMAND
UNITED STATES AIR FORCE
HANSCOM AFB, MASSACHUSETTS 01731

340794

UNCLASSIFIED

SECURITY CLASSIFICATION OF THIS PAGE (When Data Entered)

REPORT DOCUMENTATION PAGE	READ INSTRUCTIONS BEFORE COMPLETING FORM
1. REPORT NUMBER: AFGL-TR-78-0216 / 2. GOVT ACCESSION NO.: AD-A104 169	3. RECIPIENT'S CATALOG NUMBER
4. TITLE (and Subtitle): REMOTE SENSING OF ATMOSPHERIC VISIBILITY: A CRITICAL REVIEW	5. TYPE OF REPORT & PERIOD COVERED: FINAL 8 July 1977 to 30 April 1978
	6. PERFORMING ORG. REPORT NUMBER: HSS-B-041
7. AUTHOR(s): Marion P. Shuler, Jr., Harold S. Stewart	8. CONTRACT OR GRANT NUMBER(s): F19628-77-C-0202
9. PERFORMING ORGANIZATION NAME AND ADDRESS: HSS Inc, 2 Alfred Circle, Bedford, MA 01730	10. PROGRAM ELEMENT, PROJECT, TASK AREA & WORK UNIT NUMBERS: 61101F 678100 IL I ILIR7CAA
11. CONTROLLING OFFICE NAME AND ADDRESS: Air Force Geophysics Laboratory, Hanscom AFB, MA 01731, Monitor/Eric Shettle (OPA)	12. REPORT DATE: 30 April 1978
	13. NUMBER OF PAGES: 84
14. MONITORING AGENCY NAME & ADDRESS(if different from Controlling Office)	15. SECURITY CLASS. (of this report): Unclassified
	15a. DECLASSIFICATION/DOWNGRADING SCHEDULE

16. DISTRIBUTION STATEMENT (of this Report)

Approved for public release; distribution unlimited

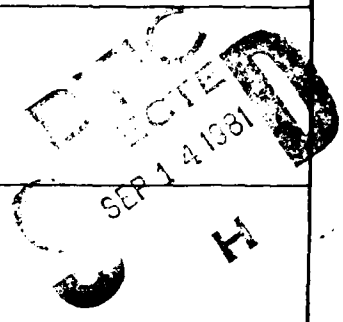

17. DISTRIBUTION STATEMENT (of the abstract entered in Block 20, if different from Report)

18. SUPPLEMENTARY NOTES

This research was supported by the Air Force In-House Laboratory Independent Research Fund.

19 KEY WORDS (Continue on reverse side if necessary and identify by block number)

Atmospheric visibility	Satellites
Atmospheric optical depth	Review
Passive remote sensing	Aerosols

20 ABSTRACT (Continue on reverse side if necessary and identify by block number)

A critical review has been made of published methods for using satellites to remotely sense the optical properties of the lower atmosphere particularly in its potential application to military photographic and electro-optical reconnaissance. The literature search was limited mainly to the archival English language publications in the optical, meteorological and environmental fields over the period 1970 to 1979. The emphasis is on passive methods which determine the total optical

DD FORM 1 JAN 73 1473

UNCLASSIFIED

SECURITY CLASSIFICATION OF THIS PAGE (When Data Entered)

20. (cont.) transmission of the atmosphere. Only three of the methods discussed have been subjected to any degree of experimental verification using satellite data.

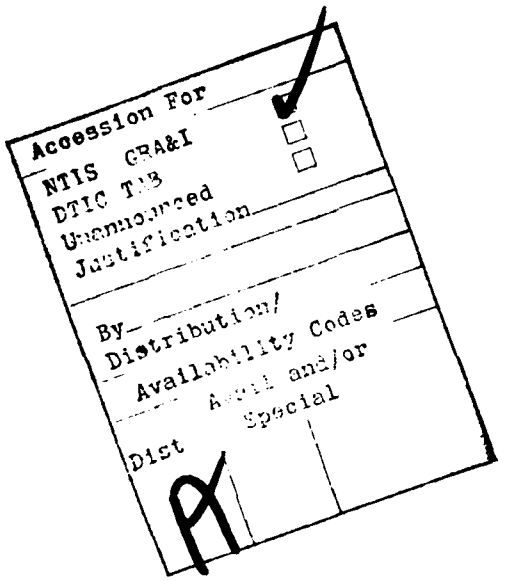

TABLE OF CONTENTS

LIST OF ILLUSTRATIONS

LIST OF ILLUSTRATIONS (Cont.)

LIST OF TABLES

REMOTE SENSING OF ATMOSPHERE VISIBILITY: A CRITICAL REVIEW

1. INTRODUCTION

1.1 Purpose

This is a final report on Contract F19628-77-C-0202, Remote Visibility Study, prepared for Air Force Geophysics Laboratory (OPA). The purpose of this study was to conduct a critical review of the published concepts for satellite based remote probing of the optical properties of the lower troposphere particularly the aerosol properties. Further the study was to assess the applicability of these and any other methods to the determination of slant path contrast reduction and atmospheric transmission for aircraft viewing geometries. These two factors control the ability of optical and electro-optical systems to detect or sense targets. Transmission affects the amount of light which reaches the system from the target while contrast reduction changes the ratio of light from the target to light from the surrounding background, i.e. the target contrast. When contrast falls below a threshold or minimum value, the system can no longer detect or see the target. The major contrast reducing agent is the aerosol in the atmospheric which scatters light into the system.

It has become common-place to use the word visibility to describe the atmospheric state as it affects the target detection capability of an electro-optical system even when the visible part of the optical spectrum is not involved. The less common term "see-ability" is more precise but still is misleading by implying a restriction to the visible spectrum. With the explicit recognition of its drawbacks, the word visibility will be used in this report for convenience.

A need for close aerial reconnaissance exists even in this age of globe-encircling reconnaissance satellites. Since the reconnaissance plane is put into considerable risk in executing its mission, it is important to have prior knowledge that the technical factors are favorable. The most

important factor is visibility conditions over the target. The military commander would have an important tool if he had the means of remotely sensing visibility. The artificial earth satellite is an obvious candidate for this purpose.

Indeed, satellites are used today in other remote sensing roles. With some degree of success, they are used to determine the vertical air temperature profile for meteorological uses. Other uses include remote assessment of geological and agricultural surface conditions. Examination of the imagery from the latter applications (Ref. 1) reveals that the presence of the earth's atmosphere distorts measurements of the radiance of surface objects and corrections must be applied to arrive at the true radiance. Since these atmospheric effects are the same that produce changes in reconnaissance visibility, there is some basis to the conjecture that satellite observations can be used to deduce surface visibilities. However, there is no direct path from these qualitative observations to the quantitative methods of measurement that are sought.

The concept of remote visibility sensing from satellites has been suggested and explored earlier by numerous investigators. Their published work has been reviewed and the most promising methods selected for presentation. Some new concepts which arose during the course of this review are also presented. Brief mention is made of some rejected methods.

1.2 Summary

The significant and practical literature on remote visibility sensing from satellites reviewed in this report covers the interval 1970 to 1979. Of course no experimental literature on this subject could have existed prior to 1958. However, the idea of using artificial earth satellites to examine the earth's atmosphere was beginning to be considered prior to Sputnik as evidenced by Reference 2 which proposes a method of determing the

vertical ozone distribution. Still by 1972, little work on visibility sensing had been published. An extensive review article on the general problem of atmospheric sensing from satellites covering up to 1972 (Reference 3) cited only four archival literature references related to particulate sensing. The literature search was based on an earlier bibliography prepared for AFGL (Reference 4) and was extended by a search in the major English language optical, meteorological, and environmental journals. Also included in this review was a series of international conferences on remote sensing in the environment.

Remote sensing of atmospheric visibility reduces essentially to detecting the amount of particulate matter in the first 5 kilometers of the troposphere. Methods can be characterized in one way by whether the illuminating source is active or passive. Active methods use lidar systems and their use over international regions might be restricted by political considerations. The applicability of active methods is summarized from more extensive studies of other researchers. The most important passive light source is the sun which can be viewed directly, by specular reflection from water surfaces, or by diffuse reflection from atmosphere and earth's surface together. Probing the atmosphere by viewing the sun directly through the atmospheric limb of the earth has only succeeded in reaching levels about 10 km above the surfaces (References 5 and 6). Thus, this concept is not applicable to this problem. Viewing the sun through specular reflection off of a water surface has been proposed as a method of measuring atmospheric transmission but no tests of the technique have been made. Most of the methods which have been tested with actual satellite data are based on measurements of the upwelling light diffusely reflected from the earth. This method is the easiest to implement but is limited to use over surfaces of low reflectance, in particular the ocean. Any method which works for the sun could be used with the moon as source as long as the measuring instruments have

sufficient sensitivity. Another possible passive source is the night illumination from cities. A method using this source is developed from a modification of the Langley method of measuring the atmospheric transmission using the sun.

The report is organized as follows: first, a brief discussion of the technical background sufficient to emphasize the major factors and to define various terms is presented. Then follows the technical discussions of the various promising techniques. Some rejected concepts are briefly mentioned. Finally, the conclusions and recommendations derived from this study are presented.

2. TECHNICAL BACKGROUND

2.1 Atmospheric Properties

The visual appearance of the atmosphere is so familiar and such a common experience that we seldom inquire deeply as to the causes of the ever changing panorama presented to our eyes. The ability to see distant objects clearly (sometimes imprecisely called visibility) changes from excellent on those brilliant clear blue sky days following the passage of a cold front to poor on those hot, humid, and hazy summer days. These changes in visibility are controlled by changes in atmospheric properties which will be described in this section. This material is given to provide the reader with the minimum background needed to read the main technical sections. A more complete review is available in "Optics of the Atmosphere" by E.J. McCartney published in 1976 (Reference 7). W.E.K. Middleton's treatise "Vision Through the Atmosphere", although published in 1952, is still a good introduction to the subject of visibility (Reference 8). Quantitative discussions of visibility will be given in Section 2.2.

The atmospheric properties that are important to visibility problems are those governing scattering and absorption of light being propagated through the atmosphere. In this context, the atmosphere is an aerosol which is defined as a dispersed system of small particles suspended in a gas. The gases are the permanent gases such as nitrogen and oxygen and the variable gases such as ozone and water vapor. The particles come from a variety of natural and man-made sources. The particle size range from 0.01 to 10 microns is important to visibility. Light scattering in gases is through the Rayleigh mechanism wherein the molecule as a classical dipole scatters the electromagnetic wave. Absorption in gases is by the molecular spectral bands which are generally in the infrared spectral region. Water

vapor and oxygen have near-infrared bands which encroach toward the visible region near 7000 Å. Water vapor bands are important insofar as they are to be avoided. Oxygen has an absorption band near 7600 Å called the A-band. The band head is at 7593 Å and the R and P branches are centered around 7619 Å. Another weaker band called the B-band is centered at 6900 Å with band head at 6867 Å. In a later section, an attempt is made to use the A-band for discriminating between an aerosol distribution smoothly decaying with height and a distribution which has a finite layer superposed on the first distribution. Ozone has a broad group of weak bands (Chappuis bands) between 5000 Å and 7000 Å which occasionally need to be considered in calculating transmittance for optical paths passing through the atmosphere. They are not further considered in this report.

Rayleigh scattering of electromagnetic waves by molecules is also valid for small particles as long as the radius is much smaller than the incident wavelength. (Near the peak of the eye sensitivity curve, light has a wavelength of 0.55 microns.) As the particle size increases, the interaction between wave and particle becomes very complex and needs the elaborate theory associated with G. Mie to describe the scattering. Since Mie scattering depends on particle size, scattering quantities for real aerosols are obtained by averaging over particle size distributions. Absorption in Mie scattering is described phenomenologically with a complex index of refraction whose imaginary part accounts for absorption.

The interaction between radiant energy in the form of electromagnetic waves and a single molecule or particle is quantitatively described in terms of a cross section. The product of this area and the power per unit area in the wavefront is the amount of power extracted from the wave by absorption or scattering. To account for a large number of molecules or particles, this cross section (dimension L^2) is multiplied by the molecular (or particle) density (dimension L^{-3}) to produce an interaction

coefficient with the dimension of an inverse length (L^{-1}). When the interaction is absorption, the result is an absorption coefficient; when the interaction is scattering, a scattering coefficient. The combination of absorption and scattering results in an extinction coefficient which is the sum of the two. These scattering coefficients are sometimes further identified as being a Rayleigh or Mie coefficient.

These symbols have to be annotated by subscripts and superscripts to indicate whether the interaction is absorption, scattering, or both (i.e. extinction) and to identify the entity (e.g. molecules, aerosols) which perturbes the optical beam. To avoid notational ambiguity, it is sometimes necessary to display what appears to be typographical excess as will be seen in Section 2.2.

Absorption interactions completely remove energy from the problem and can be described solely by an absorption coefficient. On the other hand, after a scattering event energy has not disappeared but has only been redistributed in direction. (Redistribution in wavelength can also occur but is not important to this exposition.) Since this redistribution is seldom isotropic or uniform in all directions, it is necessary to describe the amount scattered into the various directions around the scatterer. This description is made in terms of the amount of light scattered in a unit solid angle about an observing direction lying at an angle with respect to the original light beam direction. This quantity can be expressed either as an angular scattering coefficient or as an angular scattering coefficient or as the product of the total scattering coefficient, a fraction called the phase function (the term phase is an unfortunate usage which is analogous to the astronomical use of phase to mean angular aspect, as in the phases of the moon), and a normalization constant of $1/4\,\pi$. Using the same symbols with appropriate subscripts as given above to identify the specific interaction

mechanism, one can write*

$$\beta(\theta) = \beta \frac{P(\theta)}{4\pi} = \beta \Phi(\theta) \qquad (2.1)$$

In the second equality, the obvious substitution of Φ for $P/4\pi$ is made to simplify the notation. The name "phase function" will also be used for this quantity.

The scattering process is also sensitive to the polarization of the incident electromagnetic wave. Unpolarized light (of which natural sunlight is an example) can be considered to be the sum of two independent linearly polarized components of equal intensity. Thus when considering the scattering of sunlight on molecules and particles, the scattering coefficient or cross section is found by averaging the values for the parallel and perpendicular components of the beam.

Rayleigh scattering is described by a well known formula which can be used to calculate scattering coefficients for atmospheres of any known composition. Tabulations of phase function, total scattering coefficient, and angular coefficient are available to simplify Rayleigh scattering computations (see particularly References 7 and 9). The total Rayleigh scattering cross section at 0.55 microns is $\sigma_m = 4.6 \times 10^{-27}$ cm^{2}molec^{-1}. Since the number density of atmospheric molecules at sea level is 2.54×10^{19} cm^{-3}, the total scattering coefficient is $\beta_m = 1.17 \times 10^{-7}$ cm^{-1} = 11.7×10^{-3} km^{-1}. Values at other wavelengths are readily computed using the well known inverse fourth power wavelength dependence.

The calculation of Mie scattering by a single particle involves the summation of a slowly converging infinite series each term of which is a complicated function which must be evaluated on a large computer. For a mixture of particles, these calculations must be repeated many times in order to average over the particle size distribution. Needless to say,

* The symbols used in the report follow that of Ref. 7 for the most part. The reader is cautioned that this usage is not necessarily consistent with other writers.

This extensive calculation is not one to be done frequently and there is a compelling need to have tables of Mie scattering functions. Perhaps the most well known collection is that of Deirmendjian. Reference 10 which includes such diverse mixtures as water hazes, clouds, rain, and hail. The tables contain total scattering coefficients and phase functions for a wide range of wavelengths. Of particular interest are the tables for two water hazes which are representative of continental distributions (Haze C) and maritime or coastal distributions (Haze M). The tables present data on the basis of a particle size distribution of the form $n(r) = ar^{\alpha}e^{-br^{\gamma}}$ which is known as a gamma distribution. This function has enough parameters that makes it useful in fitting a wide range of observed size distributions.

The two aerosol structural characteristics, size distribution and particle density, describe the atmospheric conditions at a given point. Each of these can vary with altitude above the earth's surface but it is a standard assumption to assume that only the number density varies with altitude. This simplification allows an initial calculation to be used for cases with different particle concentrations.

Figures 2.1 through 2.3 show typical size distributions, phase functions, and extinction coefficients for a variety of models of atmospheric aerosols (Reference 11).

Extensive measurements have shown that the atmospheric aerosol is concentrated in a region near the earth's surface and that it decreases as one goes to higher altitudes. The attenuation coefficient associated with the aerosol behaves similarly; the complexity of its behavior is illustrated in Figure 2.4 which shows the vertical distribution of the attenuation coefficient at 0.55 micron wavelength. Although our concern is only with the lower four kilometers, it is interesting to see how the attenuation coefficient of the stratosphere between 15 to 25 km can vary significantly when severe volcanic eruptions throw material high into the atmosphere.

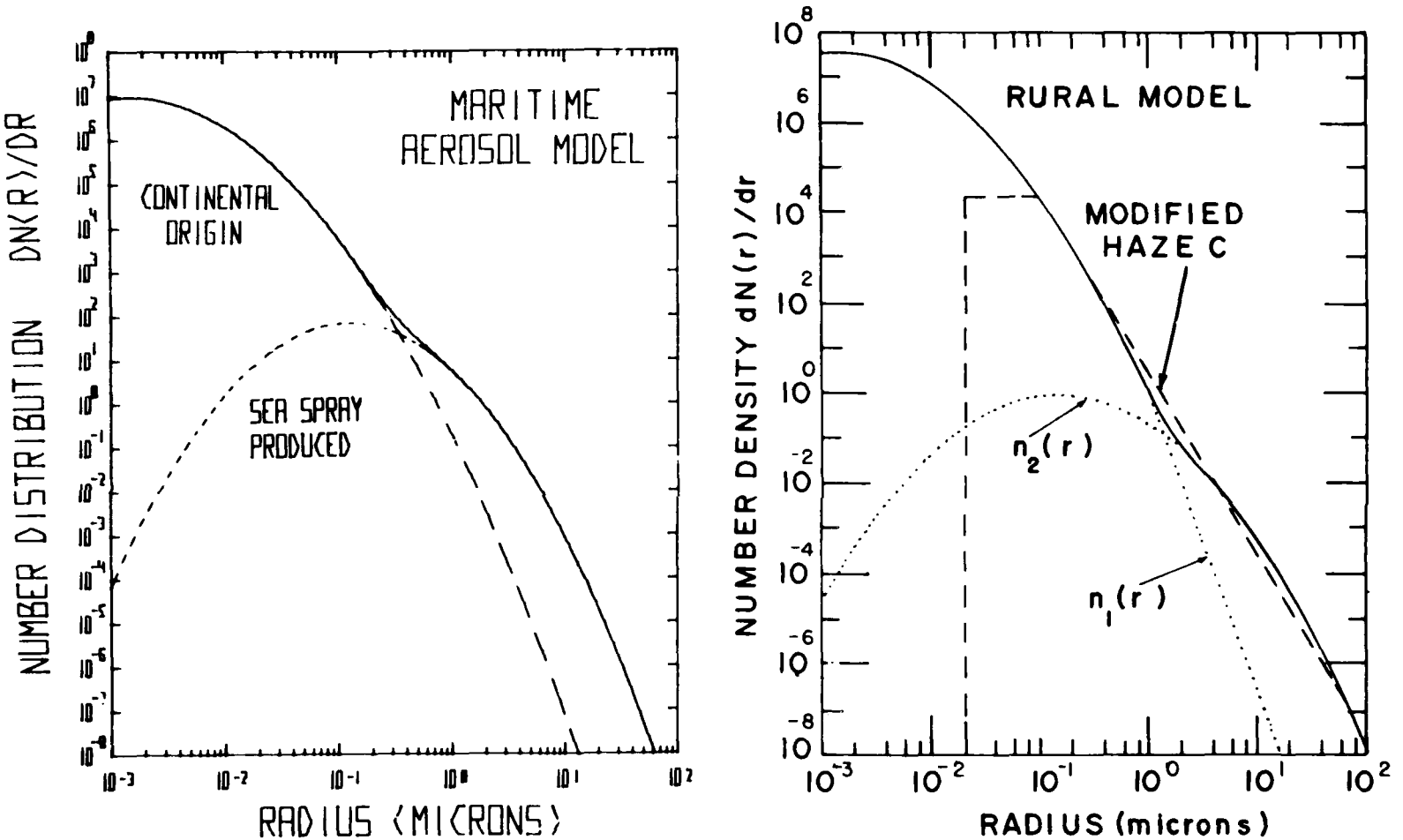

Figure 2.1. Particle size distributions for two aerosol models (from Reference 11).

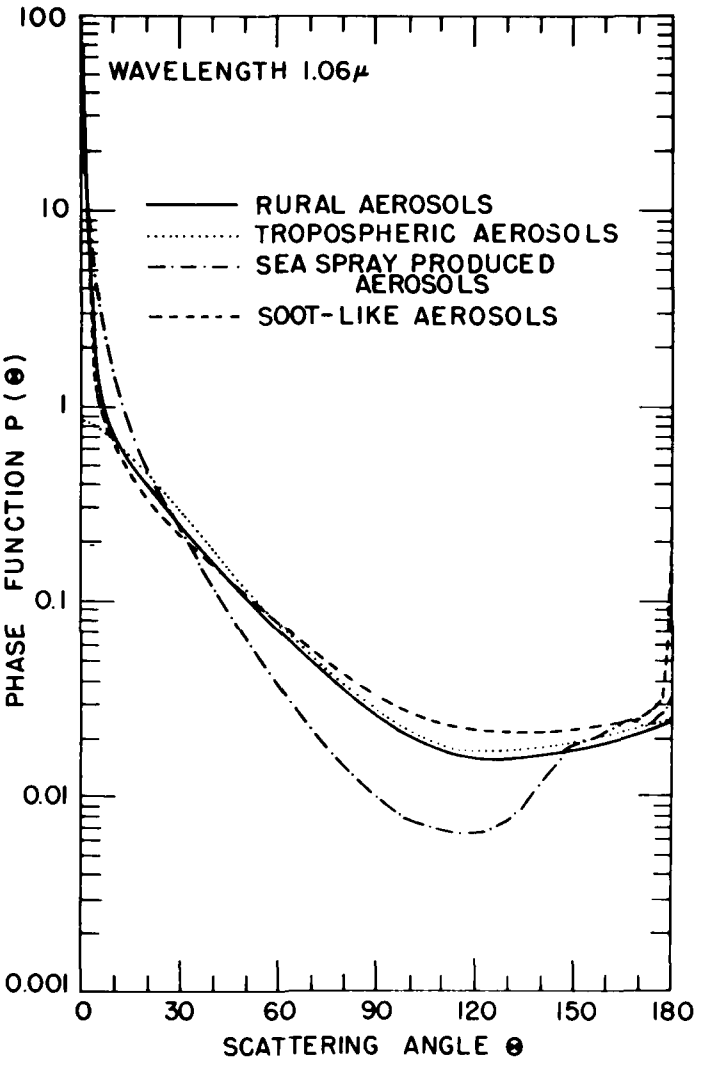

Figure 2.2. The phase function for different lower atmospheric aerosol models at a wavelength of 1.06 microns.

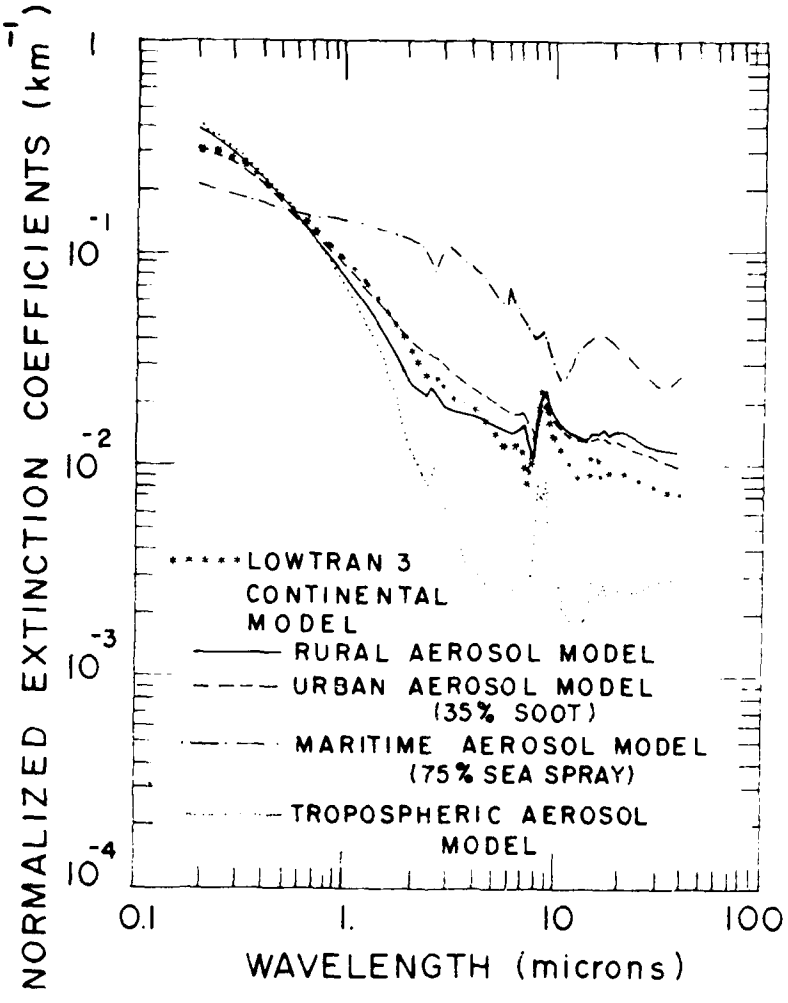

Figure 2.3. Extinction coefficients for several aerosol models (from Reference 11).

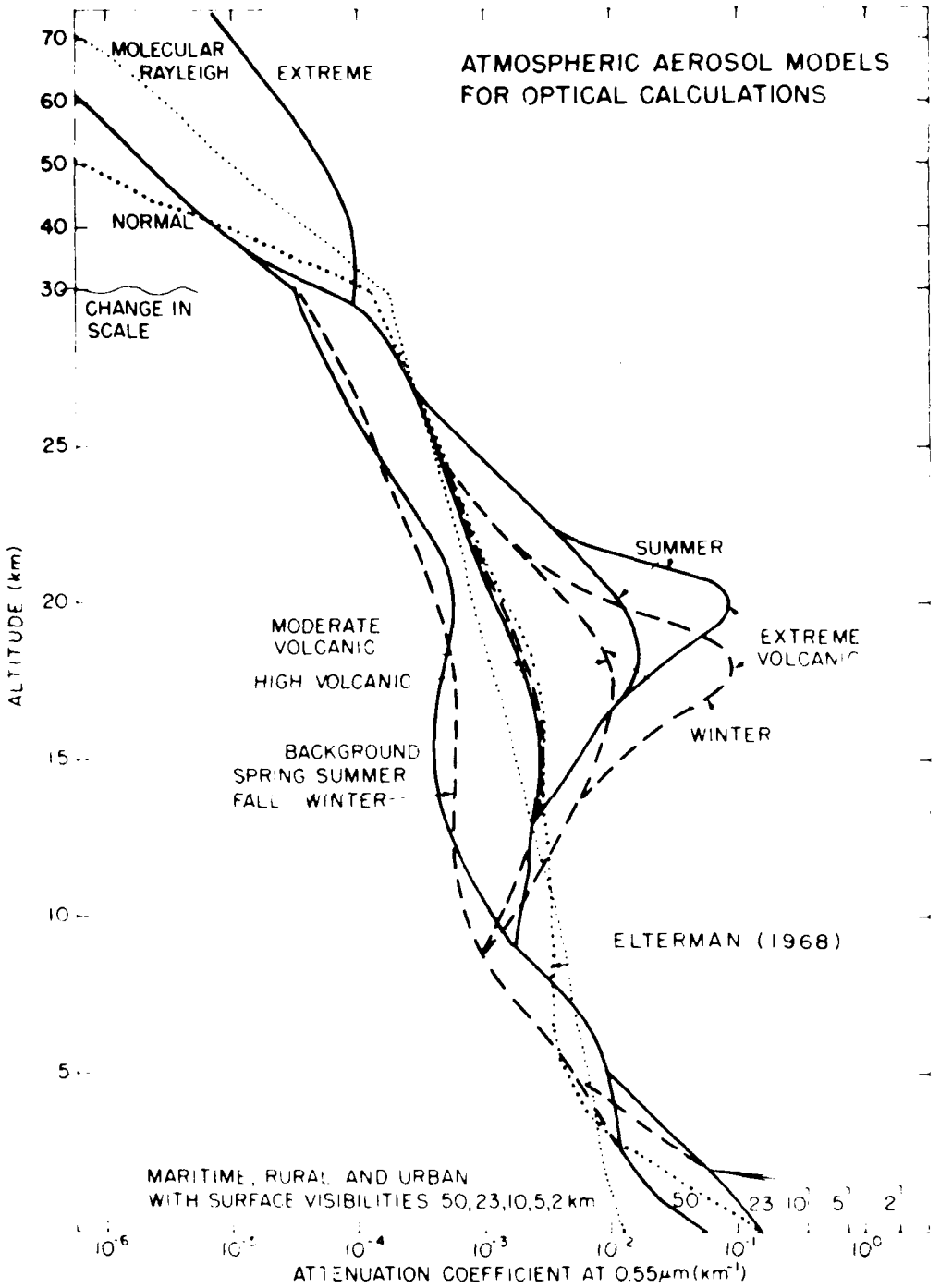

Figure 2.4. Vertical distribution of attenuation coefficient at 0.55μm wavelength for several aerosol models (from Reference 11).

The presence of temperature inversions near the surface will produce a region of nearly constant attenuation coefficient below the inversion with a sharp drop above. This behavior is usually associated with low values of meteorological visibility (e.g. 2 to 10 km as shown in Figure 2.4). In the absence of inversions, the attenuation coefficient shows a general tendency to decrease exponentially with a scale height of about 1 km as shown in Figure 2.5.

The way that these properties are used in radiation transfer problems will be shown in the next section.

2.2 Radiative Transfer

Radiative transfer theory describes the flow of radiation through matter. It finds extensive use in that part of astrophysics dealing with the escape of radiation from stars. The calculation of the brightness of the sun illuminated sky is made using the equations of radiative transfer. The theory that applies to these and other similar problems has been developed through both analytical and numerical methods. One of the classic expositions of radiative transfer is the treatise by Chandrasekhar (Reference 13) but a more readable one (but not less mathematical) is that by Sobolev (Reference 14), who provides much material on the transport of radiation in planetary atmospheres, particularly the earth. Not covered in either of these references is the Monte Carlo method which is a numerical simulation of the entire problem. A typical Monte Carlo calculation is given in Reference 15. These calculations are lengthy and therefore do not replace other numerical calculations. All of these methods of solution are too complicated to be used to make simple estimates for testing concepts. Some recent surveys of methods of solving radiative transfer problems can be found in References 16, 17, and 18. Fortunately, the problems treated in this report can be reduced to simple forms which can be calculated with not more than a programmable hand calculator.

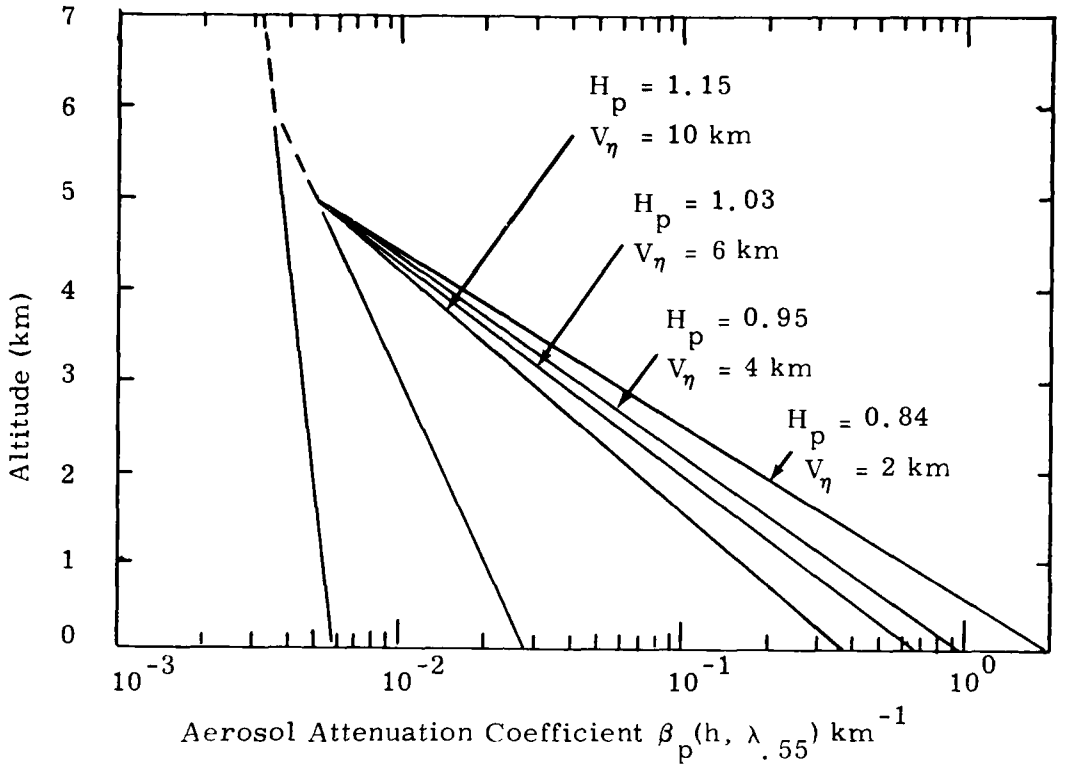

Relationships of Four Aerosol Scale Heights (H_p) With Meteorological Range (V_η), Aerosol Attenuation Coefficients (β_p) and Aerosol Mixing Layer Altitudes (0 - 5km). The aerosol scale height family was computed using $\lambda = 0.55\mu$. The dash line represents values of $\beta_p(h)$ above 5 km (Elterman, 1968)

Figure 2.5 Scheme for relating ground layer aerosol profile with meteorological range (from Reference 12).

The physical property being transported or propagated through the atmosphere is radiance, frequently called by the imprecise word brightness. This quantity is the amount of energy emitted in unit time from a unit area of a source into a unit solid angle. The cgs units are watts per cm^2 per steradian ($w\ cm^{-2} sr^{-1}$). (This quantity is called intensity in the astrophysical literature in conflict with terminology used in the physics literature.) The standard symbol used for radiance is N. If radiance is spectrally dependent, the unit wavelength or frequency interval is added to the units and the Greek minuscules λ (for wavelength) or ν (for frequency) are added to the symbol either as a subscript or in parenthesis. For example, if the spectral dependence is expressed per unit Angstrom, the spectral radiance with its units would be written $N(\lambda)$ or N_λ, ($w\ cm^{-2} sr^{-1} A^{-1}$). Radiance is the appropriate quantity to be used in most of the methods to be discussed because it pertains to extended sources and because imaging optical systems preserve radiance (except for transmission losses).

Heuristically, the equation of steady-state radiation transfer is derived by considering the change in radiance along a straight path. Changes occur when energy is lost through absorption or scattering or when energy is gained through emission from the atmosphere or from scattering of energy into the direction of the path. Self-emission of the atmosphere is only important from 3 microns and beyond. Thus only scattering is considered here.

The simplified equation of transfer can be expressed in words as follows:

[radiance change along a unit path] = [radiance decrease along unit path from absorption] + [radiance decrease along unit path from scattering] + [radiance increase along unit path from scattering]

Using the atmospheric property concepts outlined in Section 2.1, the equation of transfer can be written symbolically in the form

$$\frac{dN}{dx} = -\beta_{abs} N - \beta_{scat} N + \int \left(\beta_{scat}^{aer} \Phi_{aer}(\theta) + \beta_{scat}^{mol} \Phi(\theta) \right) N(\theta)\, d\Omega \quad (2.2)$$

The subscripted coefficients β in the first two terms on the right hand side of the equation are the total absorption and scattering coefficients for the material in the volume element around the path length dx. Each of the coefficients can be broken down into components due to the aerosol and the molecular constituents. Thus

$$\beta_{abs} = \beta_{abs}^{aer} + \beta_{abs}^{mol} \quad \text{and} \quad \beta_{scat} = \beta_{scat}^{aer} + \beta_{scat}^{mol}$$

Because of the linearity of the absorption and scattering loss terms, these coefficients can be rearranged to form extinction coefficients as follows

$$\beta_{ext}^{aer} = \beta_{abs}^{aer} + \beta_{scat}^{aer}$$

$$\beta_{ext}^{mol} = \beta_{abs}^{mol} + \beta_{scat}^{mol}$$

$$\beta_{ext} = \beta_{ext}^{aer} + \beta_{ext}^{mol}$$

Also recognizing that scattering light from molecules is by the Rayleigh mechanism, the subscripts related to that kind of scattering can be abbreviated to "Ray". Then the equation of transfer can be rewritten

$$\frac{dN}{dx} = -\beta_{ext} N + \int \left(\beta_{scat}^{aer} \Phi_{aer}(\theta) + \beta_{Ray} \Phi_{Ray}(\theta) \right) N(\theta)\, d\Phi \quad (2.3)$$

In many useful and relatively uncomplicated cases, this integro-differential equation can be simplified to a differential equation which can be easily solved. For example, by neglecting the in-scattering term, the exponential transmission formula for a collimated beam can be immediately derived, i.e.

$$N(x) = N_o e^{-(x-x_o)} \tag{2.4}$$

where N_o is the beam radiance at position x_o.

A more useful example can be obtained by considering the apparent radiance of an object having an intrinsic radiance N_o located at some distance x from the observing point in a sunlight illuminated atmosphere. On making the reasonable simplifications in Equation 2.3 that multiple scattering of light can be neglected and that an effective phase function can be used to take into account the presence of Rayleigh scattering, the following simple differential equation for the radiance along the ray path to the object is obtained.

$$\frac{dN}{dx} = -\beta_{ext} N + \beta_{scat} \Phi_{eff}(\theta) H \tag{2.5}$$

where H is the uniform solar irradiance ($W\ cm^{-2}$) on a unit path length on the ray path and θ is the scattering angle. The solution to the equation is

$$N = (\beta_{ext}/\beta_{scat}) \Phi_{eff}(\theta) H (1-e^{-\beta_{ext} x}) + N_o e^{-\beta_{ext} x} \tag{2.6}$$

When $x = o$, the radiance is correctly N_o, and when $x = \infty$, the radiance is equal to $(\beta_{ext}/\beta_{aer}) \Phi_{eff} H$ which is the radiance of the horizon seen with

with no intervening object. Thus the equation can also be written

$$N = N_H (1 - e^{-\beta_{ext} x}) + N_o e^{-\beta_{ext} x} \qquad (2.7)$$

This last equation is used to determine the visibility of objects in the atmosphere. An object is visible at a given range in the atmosphere if the difference in radiance between the object and its background exceeds some minimum difference appropriate to the detector being used. The value of the distance at which this condition holds is called the range appropriate to the detector under consideration. For example, when the eye is the detector one calls the distance the visual range.

If the contrast of an object is defined with respect to the horizon brightness behind the object, the last equation can be manipulated to give

$$N - N_H = (N_o - N_H) e^{-\beta_{ext} x} \qquad (2.8)$$

Dividing both sides by the horizon brightness one obtains an equation between the inherent contrast of the object against the background and its apparent contrast when viewed at a distance R

$$C_R = C_o e^{-\beta R} \qquad (2.9)$$

It is useful and conventional to describe the clearness of the atmosphere in terms of a distance at which objects are no longer visible. The most common such definition is that of meteorological range which is defined as that distance at which the ratio of apparent to inherent contrast at a wavelength of 0.55 microns is two percent. Thus from Equation 2.9

the meteorological range becomes

$$V_R = \frac{-\ln (0.02)}{\beta} = \frac{3.912}{\beta} \qquad (2.10)$$

This concept of contrast and contract reduction can be extended to cover more general situations where objects are viewed with respect to backgrounds other than the horizon and where contrast is relative to another object instead of the background. An application of the extended concept is discussed in Section 4.1.

3. REMOTE SENSING: GENERAL

In the context of this report, remote sensing is the measurement of atmospheric parameters from a distance. The specific concern is with measurement of atmospheric visibility and its component parameters such as particle size distribution and particle concentration from earth satellites. However, it is best to recognize at the outset that at this point in time it only appears feasible to measure the total vertical transmission of the atmosphere as a function of visible wavelengths. From the change of transmission with wavelength one can possibly infer classes of particle size distributions. Nor at this time does it seem to be feasible to measure or infer anything about the variation of any parameter with altitude above the earth's surface.

Satellites have been and are being used to measure other atmospheric parameters. The most significant of those are [illegible] temperature, vertical temperature profile, water vapor profile, ozone profile. Although the methods used to measure these parameters are generally unsuitable to the visibility problem, some aspects of the techniques will provide useful background for discussion of the visibility problem. Remote sensing techniques [illegible] of electromagnetic energy which has interacted with the atmosphere [illegible] temperature is determined [illegible]

profile is calculated by inverting an integral equation which connects the measured wavelength dependent radiance values, the Planck function of wavelength and temperature, and a weighting function varying mainly with altitude. This technique has been applied to the 15 micron IR band of CO_2. It can be used with the 5 mm microwave band of O_2. This same concept has been used to obtain vertical profiles of water vapor. In principle, the technique can be used to measure the ozone vertical profile using the 9.6 micron band; in practice the structure of the band is such that not much profile information can be obtained although the total ozone content can be measured.

Ozone distribution can be inferred by measuring the backscattered solar (or lunar) UV radiation from the atmosphere at different wavelengths in UV absorption bands. The variation in absorption changes the effective depth to which the radiation penetrates and backscatters. The changing location of effective scattering allows the variation in ozone concentration to be deduced.

Measurements on aerosols are most conveniently carried out in the wavelength region from about 0.4 to 0.9 micron. In this range, there is little absorption or emission by the particles. Thus, the possible techniques which can be used to measure visibility remotely are limited to those using the scattering of light. A simple classification scheme for these methods is illustrated schematically in Figure 3.1.

The elements of this primitive scheme are a source of light, a detector, the scattering layer whose transmission is to be measured, and a boundary which may scatter light diffusely or reflect it specularly. In the first scheme, the source and detector are on opposite sides of the scattering layer and the transmission is measured directly. The source and detector are on the same side of the layer in the second scheme, but the detector views the source through the intermediary of a specular

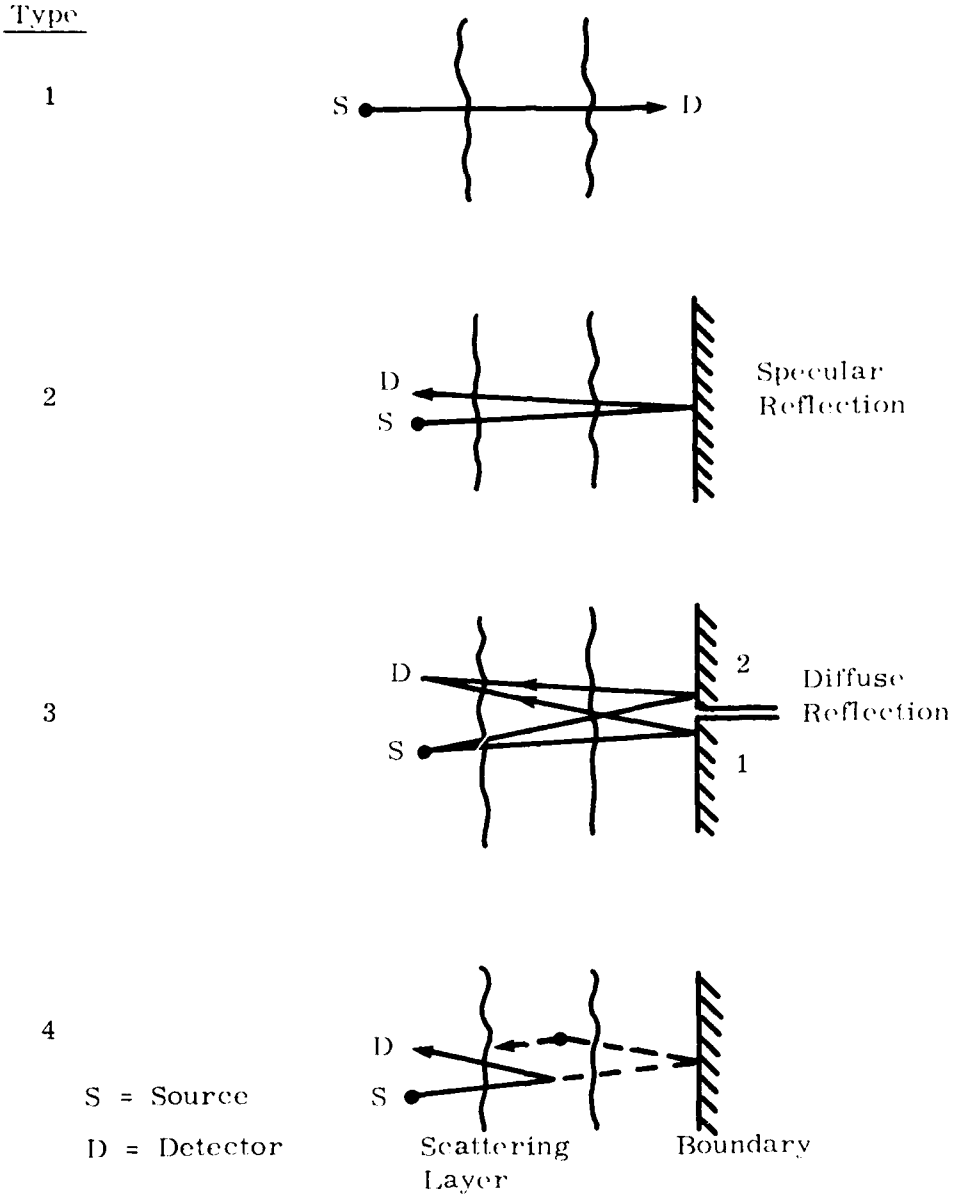

Figure 3.1. Schematic illustration of types of visibility measuring techniques.

reflector. In the third scheme, the source and detector are again on the same side, but the intermediary now becomes two diffusely reflecting surfaces with different reflectances. The quantity measured is the apparent contrast. The detector in the fourth scheme measures the backscattered light from the layer; the diffusely reflected light from the boundary surface is now an unwanted background term.

No actual scheme is as simple as these skeleton arrangements imply. For example, most actual schemes will have various background or otherwise interfering terms for which corrections must be made. Then too, the scheme must be elaborated so that enough independent measurements are made to allow for solving for the unknown variables of the problem. For example, if in a Type 1 experiment the source strength S is known, then from a single measurement D the transmission of the layer can be determined. If the source strength is unknown, then a second measurement is required. For Type 1 experiments, this additional measurement usually takes the form of an oblique view of the source through an effectively greater path. If the scattering layer is a thin gas the second transmission is equal to the perpendicular transmission raised to the power sec θ, where θ is the angle of inclination of the second path. Algebraically the two measurements are expressed

$$D_1 = T\,S_1 \quad \text{and} \quad D_2 = (T)^{\sec\theta}\,S_2 \tag{3.1}$$

Then if the source has the same value in both measurements, the transmission of the layer is

$$T = \left(\frac{D_2}{D_1}\right)^{1/(\sec\theta - 1)} \tag{3.2}$$

Rather than develop similar equations for the general types, the various specific techniques for remotely sensing atmospheric visibility will now be considered.

4. PASSIVE REMOTE SENSING

4.1 Introduction

This section presents discussions of specific methods which have been proposed in the literature for remotely measuring visibility from satellites. The technical principle of each concept is presented. Also included in the discussions are the advantages and disadvantages any any complicating features. Where it is known or readily estimated, the sensitivity is discussed. Any results or pertinent satellite experiments are extracted from the original presentation and presented.

4.2 Contrast Reduction

In Section 2.2, it was shown that contrast reduction along horizontal viewing paths in the atmosphere was directly related to the extinction coefficient. It was also stated that the concept of contrast reduction could be extended to non-horizontal paths and to a more general background. Such an extension was made by Duntley (Reference 19) and is discussed also by Middleton (Reference 8). Griggs has made this extended treatment the central concept in a method for measuring the total aerosol content of the atmosphere (Reference 20).

The idea of using a change in contrast of objects on the earth's surface to measure haze has occurred to others, for example O'Dell and Weinman (Reference 21). They predict the degradation of contrast through the use of numerical calculations of optical properties of a sunlit haze above a reflecting surface. In their approach, O'Dell and Weinman take the reflectances of two known objects along with the mean reflectance over the extended surface and find the optical thickness of the haze from a single equation and a table of derived factors. They also point out that if the optical depth is known the problem can be inverted and unknown surface reflectances determined.

Grigg's approach is similar in that he developed a model to relate optical depth of the atmosphere and the apparent contrast of the two comparison objects whose intrensic contrast is known. He did not find it necessary to account separately for a mean reflectance since he considered very large areas (the Salton Sea and the adjacent desert area). His model accounted for the solar zenith angle as did that of O'Dell and Weinman. Griggs has reported determinations of aerosol contact from ERTS-1 data taken over the test area for three days in the autumn of 1972. Lacking any concomitant ground truth data, all that can be said is that the data are reasonable.

The simplicity of the method and the (presumably) ready availability of the necessary satellite data make this method a good candidate for further exploration. An important question to be answered is how accurately must the inherent contrast of the comparison objects be known.

4.3 Upwelling Spectral Radiance

The solar radiance reflected from the earth and its atmosphere depends mainly on the surface reflectance (or albedo) and the scattering properties of the atmosphere. The atmospherically scattered radiation depends mainly on the total amount of scatterers and negligibly on their vertical distribution. Thus, it has been conjectured that in cases of low surface reflectance it would be possible to deduce the amount of aerosol in the atmosphere from measurements of the upwelling spectral irradiance from the earth-atmosphere system in conjunction with a numerical model of thephysical system. This approach using the ocean as a low reflectance surface was suggested by Griggs (References 20 & 22) who initially reported tentative tests using ERTS satellite data. Subsequentially, he has

reported further observations using data from the Landsat series satellites (Reference 23) and from the NOAA and GOES satellites (Reference 24). All of his results show over oceans there is a linear relation between the upwelling visible radiance and the atmospheric aerosol content.

A more extensive test of the concept has been reported by Koepke and Quenzel who used data from the geostationary satellite SMS taken at the time of Project GATE (Reference 25). The model radiance was calculated with a numerical method including multiple scattering and a realistic model of the ocean surface including wave structure. Figure 4.1 shows their contour plot of atmospheric turbidity in the Atlantic Ocean from the Caribbean to the African Coast on 31 July 1974. The plot also includes ground-truth measurements from stations operated for Project GATE. Figure 4.2 shows the variation of measured radiance at a fixed location (Dakar) throughout the day. Superimposed on the satellite data are calculated radiance for two aerosol models, one of which includes Sahara dust.

While this method has been demonstrated to work over oceans it does not seem to have been explored over land masses. The next logical step would be to find out whether it works over soil and vegetation regions of low reflectance. It has been suggested that some continental lakes could be used as low reflectance backgrounds (Reference 26).

4.4 Simulated Polar Nephelometer

An interesting method for obtaining the optical thickness of the earth's atmosphere from staellite based observations has been proposed by Livshits et al in Reference 28. The principle is similar to that used to obtain scattering coefficients from polar nephelometer data. If the scattering distribution function $\beta(\phi) = \beta\Phi(\phi)$ is known, then the scattering coefficient is $\beta = 2\pi\int_0^{\pi} \beta(\phi) \sin\phi \, d\phi = 2\pi\beta\int_0^{\pi} \Phi(\phi) \sin\phi \, d\phi$.

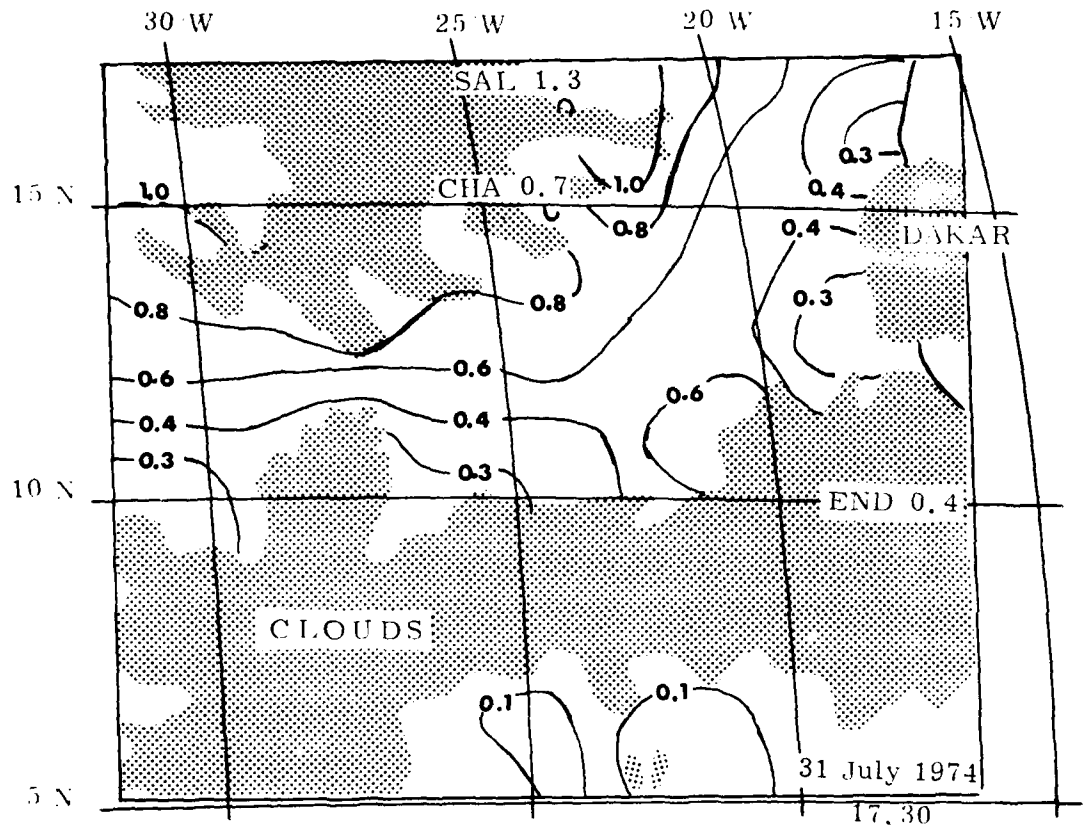

AEROSOL OPTICAL DEPTH AT 0.7μm

Version 1.12.76

Ground truth data; 30 July 74 after Prospero et al. (1976)

SAL = Sal, Cap Verde
CHA = US Ship Charterer
END = US Ship Endurer

Literature

Prospero, J.M., Carlson, T.N., Savoie, D. and Nees, R.T.(1976), Technical Report, Univ. of Miami

Figure 4.1. Contour plot of Atmospheric Turbidity determined from Geosynchronous satellite SMA (from Reference 26).

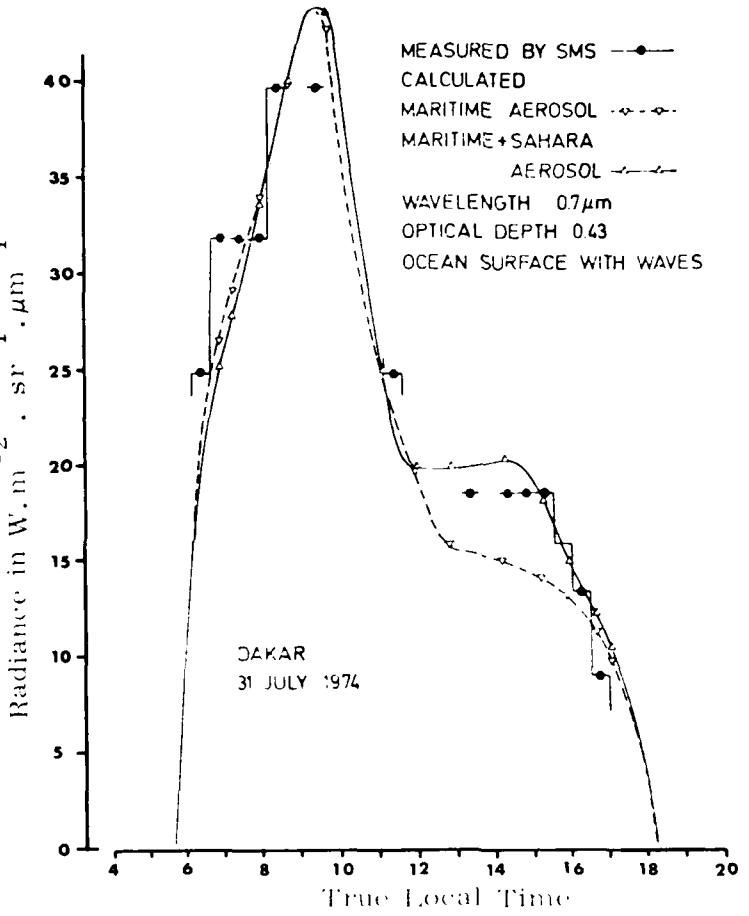

Figure 4.2. Variation of radiance at Dakar measured from geosynchronous satellite SMS (from Reference 26).

To obtain a working equation which can be used to process satellite observations, the following argument is made.

The observed scattered light intensity has components due to first-order and multiple scattering and to ground reflected light. Consider the difference of two intensities measured symmetrically about the zenith in a vertical plane through the sun. If the reflectance of the surface is symmetrical about the zenith (a weaker condition than requiring a Lambertian surface), the intensity difference contains mainly the first-order scattering component. An additional assumption which must be made is that back-scattered light at scattering angles greater than 90° can be neglected. If these assumptions hold, then the intensity difference for a given zenith angle is approximately equal to the aerosol scattering function $\beta_{aer} \Phi_{aer}(\phi)$. Measurements covering all scattering angles can then be used to find the aerosol optical thickness by integrating over the scattering angles. In practice, it is difficult to find the right conditions to make the necessary satellite observations. In particular, the important forward scatter contribution will be hard to get.

The working equation given in Reference 28 (symbols have been modified to agree with our notation) is

$$\tau_{aer} = 2\pi h \sum \left\{ \frac{(N_{1i} - N_{2i})(\tau_{aer} + \tau_R)(m_i + m_s)}{H_o \left[1 - \exp\left(-(\tau_{aer} + \tau_R)(m_i + m_s)\right) \right] m_i} - \tau_R \Delta\Phi_R \right\} \sin\phi_i \qquad (4.1)$$

The diagram in Figure 4.3 is useful in understanding the notation. N_{1i} and N_{2i} are the radiances of the earth's atmosphere observed from two directions making angles θ_i symmetrically located about the zenith. The plane containing these two directions lies in the plane formed by the zenith direction and the sun direction. The scattering angle ϕ_i is defined by the direction of radiance N_1 and the sun direction. The aerosol vertical optical thickness

of the atmosphere is τ_{aer} and the Rayleigh optical thickness τ_R. The mass of the atmosphere in the direction of the sun is m_s and in the direction of the two radiances m_i. H_o is the solar illuminance outside the atmosphere and perpendicular to the sun direction. $\Delta \Phi_R$ is the difference in the Rayleigh phase function at the two observation directions. In the form given here, the integral is approximated by a discrete sum with n points and an angular integration step h in radians. An iterative process must be used to find τ_{aer} from the given observation of radiance in units of the solar illuminance H_o and calculated values of τ_R and the phase function Φ_R.

The derivation of the working equation was not given in Reference 28 which was only a brief note. Since the source of the equation was given as an untranslated Russian reference not readily available, an independent derivation is given in Appendix A. This derivation disclosed two other implicit assumptions: (1) that β_{aer} and β_R have the same vertical altitude dependence, and (2) that the phase functions Φ_{aer} and Φ_R are constant with altitude. Neither of these are true in real atmospheres, but their effect may not be significant in practice.

This concept can also be applied to the inverse situation where observations are made from the ground. A working equation for this situation was also given in Reference 27 and appears in Appendix A as Equation A.18. Optical thicknesses obtained from this ground based method were used to calculate transparency coefficients (vertical atmospheric transmission) which were compared to transparency coefficients obtained by the Bouger method (Langley method). The correlation between the two results was good as can be seen from Figure 4.4 which is reconstructed from the original. (The optical wavelength used was not specified). Although it is not explicitly stated, it is apparent that these comparisons were used to find a correction factor to account for missing angular data.

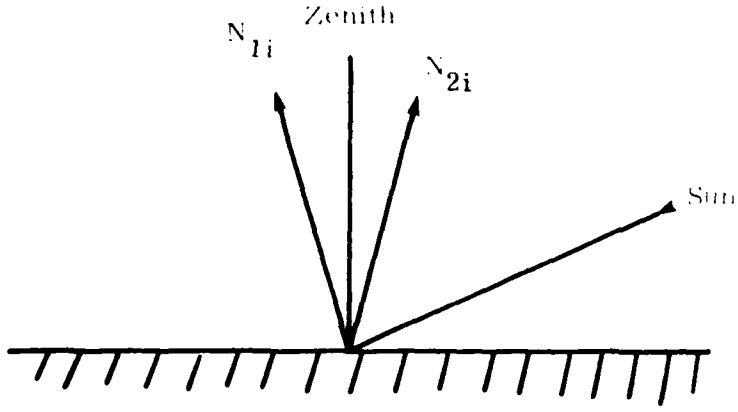

Figure 4.3. Schematic diagram of notation used in Equation 4.1.

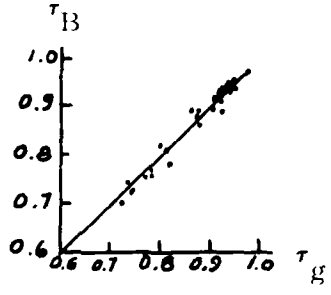

Figure 4.4. Comparison of vertical optical thickness obtained by Bouger method τ_B to values τ_g obtained by method of Equation A.18. (from Reference 28).

Data from the Kosmos 149 satellite were used to test the method given by Equation 4.1. Only those data which satisfied the following conditions were used. First, the solar zenith distance had to be large enough that an adequate range of scattering angles was obtained yet not so large that the earth's curvature effects were significant. A solar zenith distance of 75° was found to be suitable. Second, the measurements had to be in (or near) the plane of the sun's vertical. Finally, only data from a cloudless atmosphere were valid.

Data satisfying all of these criteria were used with the working equation to find a value of optical thickness which was then corrected by an empirical correction factor that had been previously determined by comparisons between other values determined by this method and ground measurements of the Bouger optical thickness (vertical atmospheric thickness determined by Langley method). No ground truth data was available to validate these results. The authors state that the histogram of optical thicknesses obtained from the satellite technique was similar to those obtained in ground measurements. They further add that the results suggest that the asymmetry of the reflected light had little influence on the determination, in agreement with the assumption.

In spite of the several assumptions whose validity can be questioned, this method is potentially important in that it removes the ground reflectance from the problem. At the same time the technique of subtracting two measurements is its main weakness, since the residual difference must be greater than noise and instrumental fluctuations in the two symmetrical measurements. In practice, this restriction will limit measurements to regions of low but finite reflectance.

4.5 Nighttime Observations of Cities*

The vertical optical thickness of the earth's atmosphere is frequently determined from ground-based stations by a technique called the Langley method in American literature and the Bouger method in European literature. A photometer is aimed at the sun and its output is recorded as a function of the sun's zenith angle. Using the approximation that the path through the atmosphere is proportional to the secant of the zenith angle for angles less than 80 degrees, the output signal is

$$S = S_o e^{-\tau_o \sec\theta} \tag{4.2}$$

and the natural logarithm of the signal is

$$\ln S = \ln S_o - \tau_o \sec\theta \tag{4.3}$$

or the common logarithm

$$\log S = \log S_o - \tau_o \sec\theta \log e \tag{4.4}$$

$$= \log S_o - 0.4343\ \tau_o \sec\theta$$

A plot of the common log of the output against sec θ is a straight line whose intercept is $\log S_o$ and slope is $(-0.4343\ \tau_o)$. The vertical thickness of the atmosphere τ_o can be calculated from the slope.

This method could be reversed if there were isotropic light sources on the ground. The illumination of modern cities at night is intense enough to be detected but is most certain not to be isotropic. Excellent photographs of the nighttime earth can be found in References 29 and 30.

*The concept in this section developed during discussions with E. Shettle of an earlier idea.

The angular variation of the un-resolved light source can be resolved into Fourier components which will not be known a priori but might possibly be determined from the data.

To examine the feasibility of this concept, a hypothetical source composed of an isotropic source and a cosine varying source in different proportions will be investigated. The intensity of the source as observed from outside the earth's atmosphere as a function of zenith angle will be

$$J(\tau_o,\theta) = (a + b\cos\theta)\, e^{-\tau_o \sec\theta} \qquad (4.5)$$
$$= a\left(1 + \frac{b}{a}\cos\theta\right) e^{-\tau_o \sec\theta}$$
$$= a(1 + c\cos\theta)\, e^{-\tau_o \sec\theta}$$

By normalizing to the value at the vertical and writing $\cos\theta = u$, the expression becomes

$$j(\tau_o,u) = \frac{a(1 + cu)\, e^{-\tau_o/u}}{a(1+c)\, e^{-\tau_o}} \qquad (4.6)$$
$$= \left(\frac{1}{1+c} + \frac{c}{1+c}u\right) e^{-\tau_o\left(\frac{1}{u} - 1\right)}$$

Further mathematical manipulation can put this relation in a more convenient form. Let $c/(1+c) = d$ and $1/(1+c) = 1 - d$. Also let $w = \left(\frac{1}{u} - 1\right) = (1-u)/u$. Then $j(\tau_o, w) = \left[1 - d\left(\frac{w}{w+1}\right)\right] e^{-\tau_o w}$. The constant d measures the proportion of cosine variation in the source and ranges from zero to unity. When the zenith angle varies from 0° to 85°, the variable w ranges from 0 to 10. Figures 4.5 to 4.7 show how the normalized intensity varies as a function of angle through the variable w for different values of the vertical optical thickness τ_o. The parameter d varies from curve to curve. Since examination of these graphs does not reveal any obviously simple way of recovering the two unknown quantities τ_o and d, numerical methods must be used.

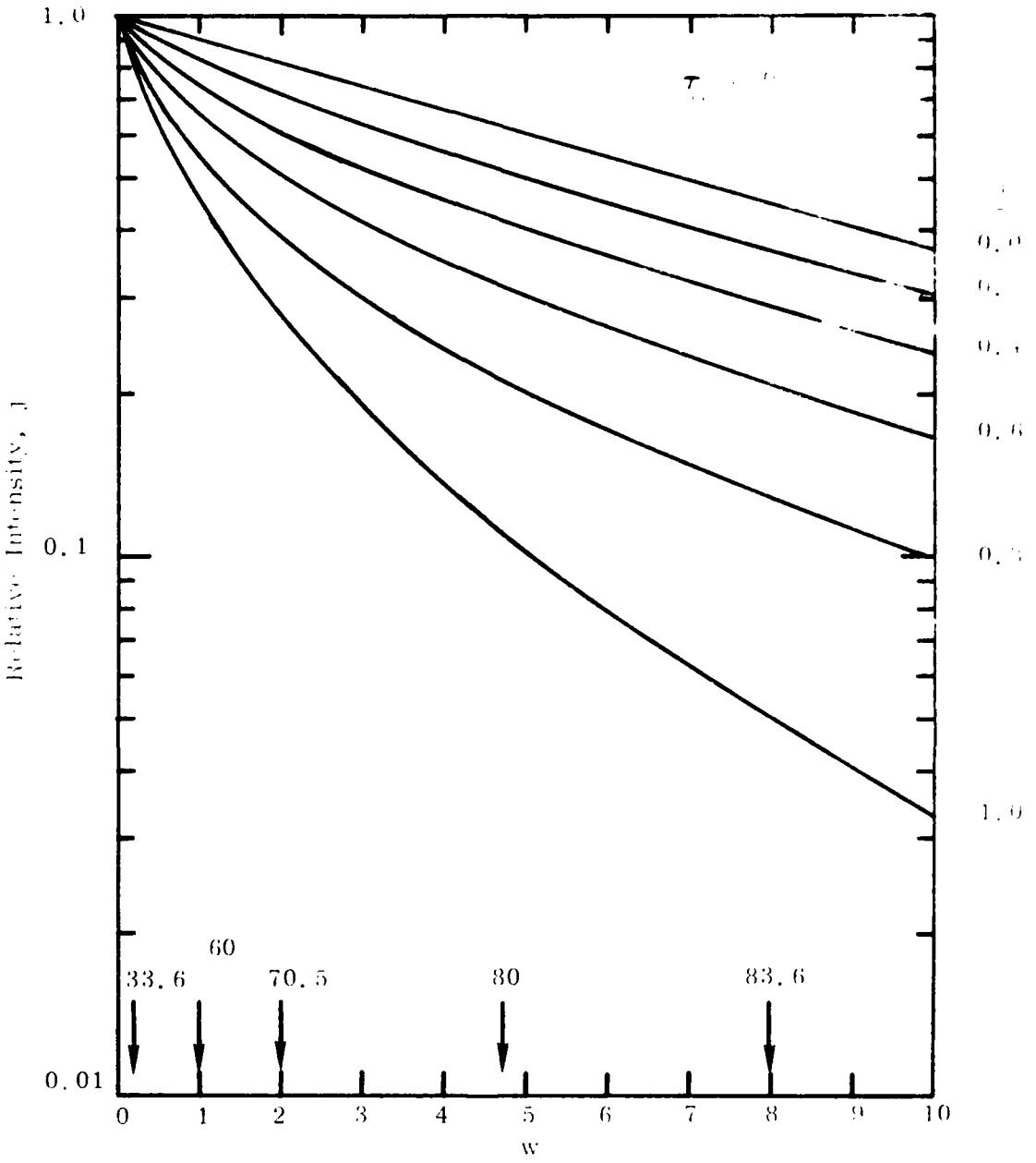

Figure 4.5. Normalized intensity variations with zenith angle of combined isotropic and cosine varying sources observed outside an atmosphere of optical thickness 0.1. See Eq. 4.6 for definition of a.

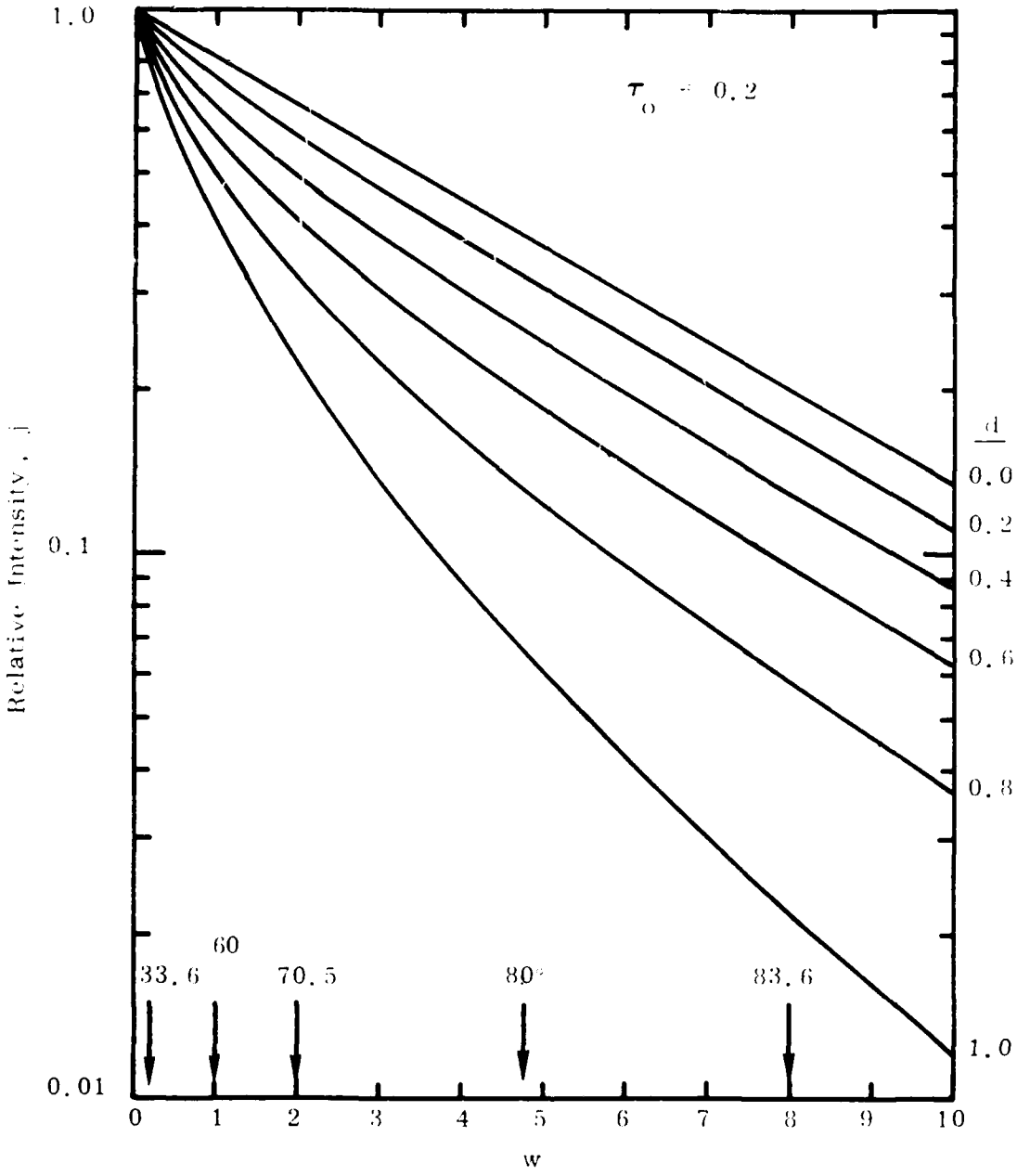

Figure 4.6. Normalized intensity variations with zenith angle of combined isotropic and cosine varying sources observed outside an atmosphere of optical thickness 0.2. See Eq. 4.6 for definition of d.

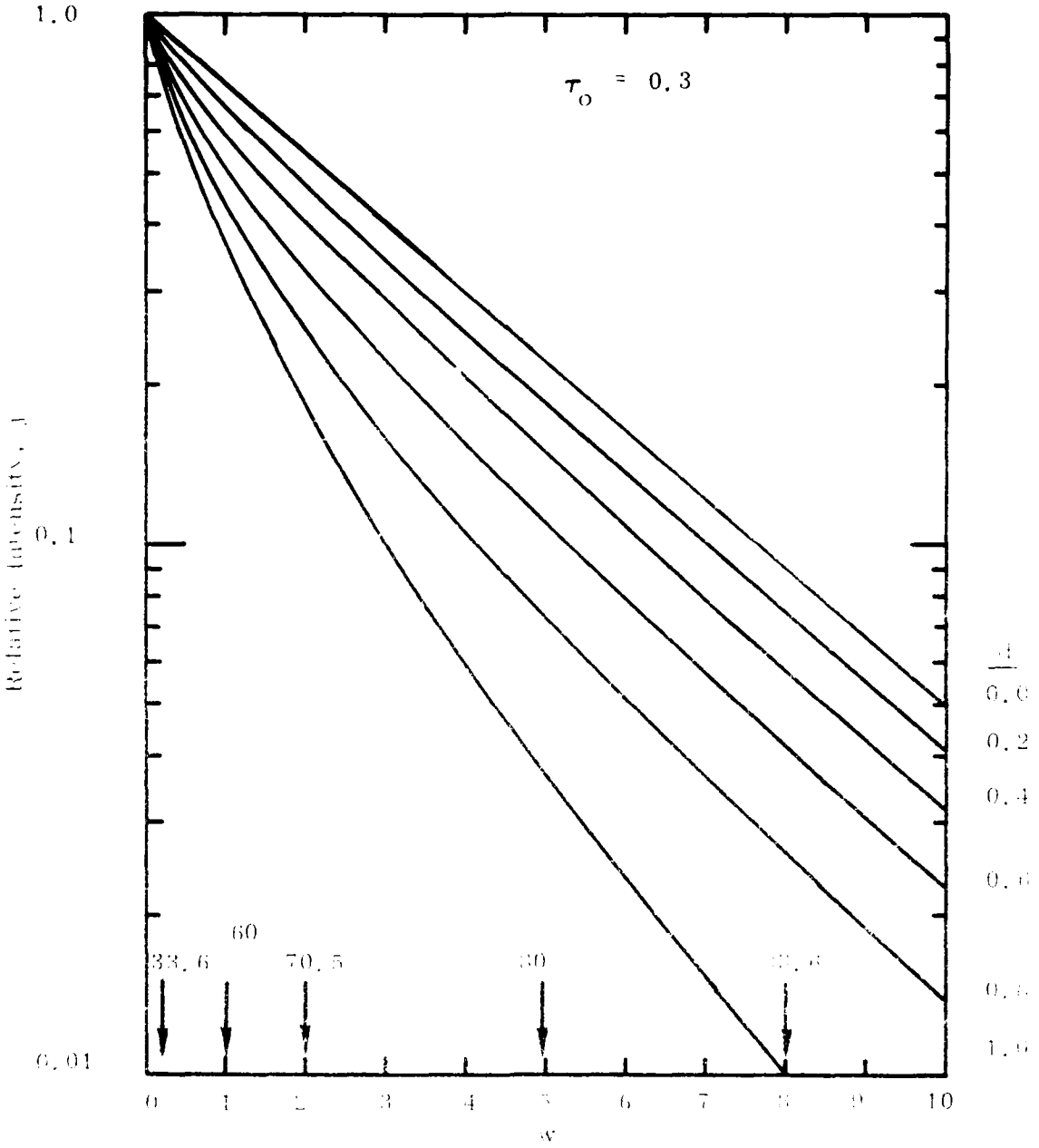

Figure 4.7. Normalized intensity variations with zenith angle of combined isotropic and cosine varying sources observed outside an atmosphere of optical thickness 0.3. See Eq. 4.6 for definition of d.

The working equation giving the measured intensity as a function of w, τ_o and d can be alternately solved for τ_o and d

$$e^{\tau_o} = \left[\frac{1}{j}\left(1 - d\frac{w}{w+1}\right)\right]^{\frac{1}{w}} \tag{4.7}$$

$$d = \frac{w+1}{w}\left[1 - j e^{\tau_o w}\right] \tag{4.8}$$

If the intensity is measured at two different angular positions, a simple iterative numerical process (described in Appendix B) can be used to solve for τ_o and d. This procedure has been used to estimate the precision to which these values can be determined. The exact values of j are systematically varied by $\pm$ 1 percent, and these perturbed values then used to calculate values of τ_o and d. Table 4.1 shows the resulting variations in these values. Since the variations appear to be linear, assumed variations of $\pm$ 5 percent in the measured intensities would cause variations in the calculated τ_o and d to be five times as great. Thus, in the worst case, there will be an error of about 30 percent in the value of vertical optical thickness deduced from a pair of measurements. This error can be reduced by averaging the results of many pairs of measurements. Although this analysis needs to be extended to additional terms in the Fourier expansion, it shows considerable promise at this point.

It is probable that the intensity and angular distribution of light from a given city remains approximately the same from night to night. In that case, the city would have characteristic values of "j_o" and "d" for each hour of the night (excluding perhaps deviations resulting from night baseball or football games, major fires, etc.). Such characteristic values could be used as initial guesses in the iterative solution or even as the basis for estimating the optical depth from a single measurement.

Table 4.1 Calculated variations in deduced values of τ_o and d resulting from ± 1 % variations in observed intensity values for different true values of τ_o and d.

τ_o	d			
	0.2		0.8	
	τ_o	d	τ_o	d
0.2	± 2 %	± 12 %	± 6 %	± 4 %
0.8	± 6 %	± 11 %	± 2 %	± 3 %

4.6. Reciprocal Observations of Differences in Brightness

In section 4.2, a method for obtaining the transmission of the atmosphere by measuring the reduction in contrast of two areas on the earth with different reflectivity was described. It is a Type 3 method in our simple classification scheme and requires a single observation along with a prior knowledge of the two reflectances. This method is generalized in this section to get a method which does not need values of reflectances, but at the price of complexity in number and condition of observations.

A surface, a, is irradiated by attenuated direct sunlight and forward scattered sunlight. The direct term is

$$H_o \cos \phi_1 e^{-\tau \sec \phi_1} \tag{4.9}$$

where ϕ_1 is the zenith angle of the sun and τ is the optical depth of the atmosphere evaluated along the vertical,

The forward scattered radiation reaching the surface is

$$H_o (1 - e^{-\tau \sec \phi_1}) R (\phi_1) \cos \phi_1 \tag{4.10}$$

where $(1-e^{-\tau \sec \phi_1})$ is the total of scattered light and $R (\phi_1)$ is the fraction of that total which is scattered in a downward direction.

The inherent radiance of the surface $N_a^* (\phi_1 \phi_2)$ when viewed at angle ϕ_2 (measured from the zenith) is

$$N_a (\phi_1 \phi_2) = H_o \cos \phi_1 [\rho_a f_a (\phi_1 \phi_2) e^{-\tau \sec \phi_1} + \rho_a g_a (\Omega_1 \phi_2) \cdot (1 - e^{-\tau \sec \phi_1}) R (\phi_1)] \tag{4.11}$$

where ρ_a is the reflectivity of surface a and $\rho_a f_a (\phi_1 \phi_2)$ is the probability that a photon incident at angle ϕ_1 will be scattered into an element of solid angle in the direction ϕ_2 (sr^{-1}) and $\rho_a g_a (\Omega_1 \phi_2)$ is the probability that forward scattered radiation incident on the surface will be scattered into an element of solid angle in the direction ϕ_2 (sr^{-1}).

The apparent radiance of the surface $N_a(\phi_1\phi_2)$ when viewed from outside the atmosphere is

$$N_a(\phi_1\phi_2) = N_a^* e^{-\tau \sec \phi_2} + U(\phi_1\phi_2) \tag{4.12}$$

$$N_a(\phi_1\phi_2) = H_o \cos\phi_1 e^{-\tau \sec \phi_2} [\rho_a f_a(\phi_1\phi_2) e^{-\tau \sec \phi_1} + \rho_a g_a(\Omega_1\phi_2) \cdot (1-e^{-\tau \sec \phi_1}) R(\phi_1)] + U(\phi_1\phi_2) \tag{4.13}$$

where $U(\phi_1\phi_2)$ is the upwelling light which has been scattered in the atmosphere.

The apparent radiance of a second surface, b, adjacent to a may be described as follows:

$$N_b(\phi_1\phi_2) = H_o \cos\phi_1 e^{-\tau \sec \phi_2} [\rho_b f_b(\phi_1\phi_2) e^{-\tau \sec \phi_1} + \rho_b g_b(\Omega_1\phi_2) \cdot (1-e^{-\tau \sec \phi_1}) R(\phi_1)] + U(\phi_1\phi_2) \tag{4.14}$$

The brightness difference between surfaces a and b when illuminated from ϕ_1 and viewed from ϕ_2 is $D_{ab}(\phi_1\phi_2)$ where,

$$D_{ab}(\phi_1\phi_2) = H_o \cos\phi_1 [e^{-\tau(\sec\phi_1 + \sec\phi_2)} \{\rho_a f_a(\phi_1\phi_2) - \rho_b f_b(\phi_1\phi_2)\} + (1-e^{-\tau \sec\phi_1}) e^{-\tau \sec\phi_2} R(\phi_1) \{\rho_a g_a(\Omega_1\phi_2) - \rho_b g_b(\Omega_1\phi_2)\}] \tag{4.15}$$

The brightness difference between surfaces a and b when illuminated from ϕ_2 and viewed from ϕ_1 is $D_{ab}(\phi_2\phi_1)$ where,

$$D_{ab}(\phi_2\phi_1) = H_o \cos\phi_2 [e^{-\tau(\sec\phi_1 + \sec\phi_2)} \{\rho_a f_a(\phi_2\phi_1) - \rho_b f_b(\phi_2\phi_1)\} + (1-e^{-\tau \sec\phi_2}) e^{-\tau \sec\phi_1} R(\phi_2) \{\rho_a g_a(\Omega_2\phi_1) - \rho_b g_b(\Omega_2\phi_1)\}] \tag{4.16}$$

The coefficients $f_a(\phi_1\phi_2)$ and $f_b(\phi_1\phi_2)$ as used here meet the requirements

of the reciprocity theorem and hence

$$f_a(\phi_1\phi_2) = f_a(\phi_2\phi_1) \tag{4.17}$$

$$f_b(\phi_1\phi_2) = f_b(\phi_2\phi_1) \tag{4.18}$$

Now

$$D_{ab}(\phi_1\phi_2)\cos\phi_2 - D_{ab}(\phi_2\phi_1)\cos\phi_1 =$$
$$H_o\cos\phi_1\cos\phi_2[(1-e^{-\tau\sec\phi_1})e^{-\tau\sec\phi_2}R(\phi_1)\{\rho_a g_a(\Omega_1\phi_2)-\rho_b g_b(\Omega_1\phi_2)\} -$$
$$(1-e^{-\tau\sec\phi_2})e^{-\tau\sec\phi_1}R(\phi_2)\{\rho_a g_a(\Omega_2\phi_1)-\rho_b g_b(\Omega_2\phi_1)\}] \tag{4.19}$$

So far no assumptions have been made. To go further requires some relationships between $R(\phi_1)$ and $R(\phi_2)$, between $g_a(\Omega_1\phi_2)$ and $g_a(\Omega_2\phi_1)$ and between $g_b(\Omega_1\phi_2)$ and $g_b(\Omega_2\phi_1)$.

The coefficient $R(\phi)$ has to do with the scattering of sunlight incident from zenith angle ϕ. $R(\phi)$ is the fraction of the scattered sunlight which continues in a downward direction. This fraction is a function of the zenith angle ϕ. If a model for the scattering process is assumed, for instance, Rayleigh scattering plus an appropriate quantity of a continental aerosol as described by Deirmendjian then, for any value of τ, the optical depth of the vertical atmosphere, the quantity of aerosol is fixed and $R(\phi)$ can be calculated easily for all values of (ϕ) as long as single scattering dominates. In cases for which aerosol scattering is reasonably greater than molecular scattering, which is always the case for the red end of the visible spectrum and usually the case for the total visible spectrum except in very clear weather, the ratio $R(\phi)$ can be fixed for any value of ϕ without regard to τ. At this stage it is assumed that this is the case and values of $R(\phi)$ can be assigned. A first cut at calculating $R(\phi)$ is presented in Appendix C.

The coefficients such as $g_a(\Omega_1 \phi_2)$ have to do with the probability that a photon incident on surface a from a direction within the solid angle Ω_1 with central axis in the direction ϕ_1, will be scattered into an element of solid angle in the direction ϕ_2. The distribution about ϕ_1 of the numbers of photons within Ω_1 will be quite similar to the phase function for scattering and will have a strong forward lobe. With this in mind one can write

$$g_a(\Omega_1 \phi_2) \approx g_a(\Omega_2 \phi_1) \tag{4.20}$$

since the conditions for reciprocity are approached but not met. If the surface a is Lambertian then,

$$\rho_a g_a(\Omega_1 \phi_2) = \rho_a g_a(\Omega_2 \phi_1) = \frac{\rho_a}{\pi} \tag{4.21}$$

where ρ_a is the reflectivity of the surface a. In what follows it will be assumed that $g_a(\Omega_1 \phi_2) = g_a(\Omega_2 \phi_1)$ for whatever reason. At this stage equation 4.21 will be used.

Equation 4.19 can now be rewritten

$$D_{ab}(\phi_1 \phi_2) \cos \phi_2 - D_{ab}(\phi_2 \phi_1) \cos \phi_1 = \tag{4.22}$$

$$H_o \cos \phi_1 \cos \phi_2 \left(\frac{\rho_a - \rho_b}{\pi}\right) \{ R(\phi_1) (1 - e^{-\tau \sec \phi_1}) e^{-\tau \sec \phi_2} - R(\phi_2) (1 - e^{-\tau \sec \phi_2}) e^{-\tau \sec \phi_1} \}$$

Now imagine that a second pair of observations are made involving angles ϕ_3 and ϕ_4

$$D_{ab}(\phi_3 \phi_4) \cos \phi_4 - D_{ab}(\phi_4 \phi_3) \cos \phi_3 =$$

$$H_o \cos \phi_3 \cos \phi_4 \left(\frac{\rho_a - \rho_b}{\pi}\right) \{ R(\phi_3) (1 - e^{-\tau \sec \phi_3}) e^{-\tau \sec \phi_4} - R(\phi_4) (1 - e^{-\tau \sec \phi_4}) e^{-\tau \sec \phi_3} \} \tag{4.23}$$

and finally

$$\frac{D_{ab}(\phi_1\phi_2)\cos\phi_2 - D_{ab}(\phi_2\phi_1)\cos\phi_1}{D_{ab}(\phi_3\phi_4)\cos\phi_4 - D_{ab}(\phi_4\phi_3)\cos\phi_3} = \frac{\cos\phi_1\cos\phi_2}{\cos\phi_3\cos\phi_4}\left[\frac{R(\phi_1)(1-e^{-\tau\sec\phi_1})e^{-\tau\sec\phi_2} - R(\phi_2)(1-e^{-\tau\sec\phi_2})e^{-\tau\sec\phi_1}}{R(\phi_3)(1-e^{-\tau\sec\phi_3})e^{-\tau\sec\phi_4} - R(\phi_4)(1-e^{-\tau\sec\phi_4})e^{-\tau\sec\phi_3}}\right] \quad (4.24)$$

One notes that the left hand side of equation 4.24 involves measurable quantities and the right hand side involves only one unknown, τ. In principle, then, if the assumptions made are acceptable, the optical depth of the vertical atmosphere can be calculated from four measurements of the difference in brightness of two adjacent areas on the earth's surface. These measurements are not made casually. Exacting relationships to the solar zenith angles are defined by the conditions discussed in the text above.

A variation on the method is of some interest. Imagine that the surface a is of great extent and the surface b is small and well within the boundaries of a. For example, a might extend beyond b at least 10 times h, the scale height of the aerosols ($h \approx 1$ km) and b, while resolvable, might have no dimension greater than 0.2h. Under these conditions b is a small perturbation in a. If in the atmosphere above the surface all gradients in scattering effects are vertical (an assumption made throughout this section) then for regions of a a few kilometers in from its edges the reciprocity principle will hold for the combination surface plus atmosphere. That is

$$N_a(\phi_1\phi_2)\cos\phi_2 = N_a(\phi_2\phi_1)\cos\phi_1$$

$$N_a(\phi_3\phi_4)\cos\phi_4 = N_a(\phi_4\phi_3)\cos\phi_3 \quad (4.25)$$

The left hand side of equation 4.24 may be written

$$\frac{\{N_a(\phi_1\phi_2) - N_b(\phi_1\phi_2)\}\cos\phi_2 - \{N_a(\phi_2\phi_1) - N_b(\phi_2\phi_1)\}\cos\phi_1}{\{N_a(\phi_3\phi_4) - N_b(\phi_2\phi_4)\}\cos\phi_4 - \{N_a(\phi_4\phi_3) - N_b(\phi_4\phi_3)\}\cos\phi_3}$$

using equations 4.25 this becomes

$$\frac{N_b(\phi_1\phi_2)\cos\phi_2 - N_b(\phi_2\phi_1)\cos\phi_1}{N_b(\phi_3\phi_4)\cos\phi_4 - N_b(\phi_4\phi_3)\cos\phi_3}$$

This, now, may be set equal to the right hand side of equation 4.24. In this interesting case only the brightness of the small patch b must be measured from four positions to obtain τ. Again these positions and their relationships to the zenith angle of the sun are established in a rather exacting way by the foregoing text.

The observing position requirements cannot be satisfied by a single orbiting satellite progressing in same direction as the sun. While it may not be cost effective to devote multiple satellites to routine observation of visibility, this method might be employed for one-time calibration or comparison purposes. It could also be used in those fortuitous cases where the observing positions occur with existing satellites in orbit.

4.7 Upwelling Spectral Radiance Observed in Oxygen A Band

A major source of difficulty in attempting to measure the amount of atmospheric aerosol from the upwelling spectral radiance as discussed in Section 4.3 is the presence of light reflected from the earth's surface. The methods given in Section 4.3 were limited to conditions where this component of the measured light was small and was accounted for through a model of the process. The method of Section 4.4 eliminates the ground reflection by subtracting two signals, one of which is essentially the background reflection. The possibility of eliminating the background by absorption is explored in this Section. Since the proposed method does not appear to have sufficient sensitivity, only an outline of the concept and the final results are presented.

It was mentioned in Section 2.1, that oxygen molecules have an absorption band with origin at 0.7619 microns. If the earth is observed in narrow spectral resolution through this band, then different amounts of total path absorption will occur as different parts of the band are used. And since the surface and the aerosol scatterers are located at different places on the light path, the contributions of each to the reflected light should be weighted differently. In principle then, it might be possible to separate out the surface reflectance.

To investigate this concept, the following simple problem was set up and evaluated on a HP-19C programmable calculator. Radiation from the sun is incident on the earth's atmosphere and surface at a given zenith angle. The single scattered reflected spectral radiance is calculated at various narrow intervals in the oxygen A-band. It is further assumed that strong forward scattering effectively eliminates any scattering extinction effects for both the incoming solar flux and the upwelling single

scattered flux. The Elterman model for different surface meteorological ranges (Reference 12 and Figure 2.5) was used to describe the atmospheric aerosol. Calculations were made for one surface reflectance (15 percent) two viewing configurations and two surface meteorological ranges (5 km and 20 km).

Figure 4.8 shows the results with sun at 45° zenith angle and the observer at the zenith, while Figure 4.9 shows results with the sun again at 45° but with the observer now at 90° with respect to the sun. Each graph shows the total radiance N and its components from the aerosol, N_{aer}; Rayleigh scattering, N_R; and the ground N_G. The range of absorption coefficient is sufficient to reach the bottom of the absorption band. Although there is a calculational difference between the two visibility conditions, it does not appear to be large enough to distinguish between them.

It is possible that over oceans when the surface reflectance is small, then some vertical resolution of the atmospheric attenuation may be achieved by this method. However, over land where surface albedos range from 0.1 to 0.5 for surface areas and up to 0.9 over clear snow, the expectation of achieving any vertical resolution is not high. Further complications arise because the 0.76 micron band falls within the high reflectivity chlorophyll band and strong seasonal variations in surface reflectivity can be expected.

Subsequent to our analysis, Badayev and Malkevich published a paper describing a similar concept (Reference 34) but using a more sophisticated mathematical approach. They consider the method to be useful over weakly reflecting surfaces on the basis of their numerical calculations. Also they appear to be more optimistic about making corrections for multiple scattering and finite surface reflectances.

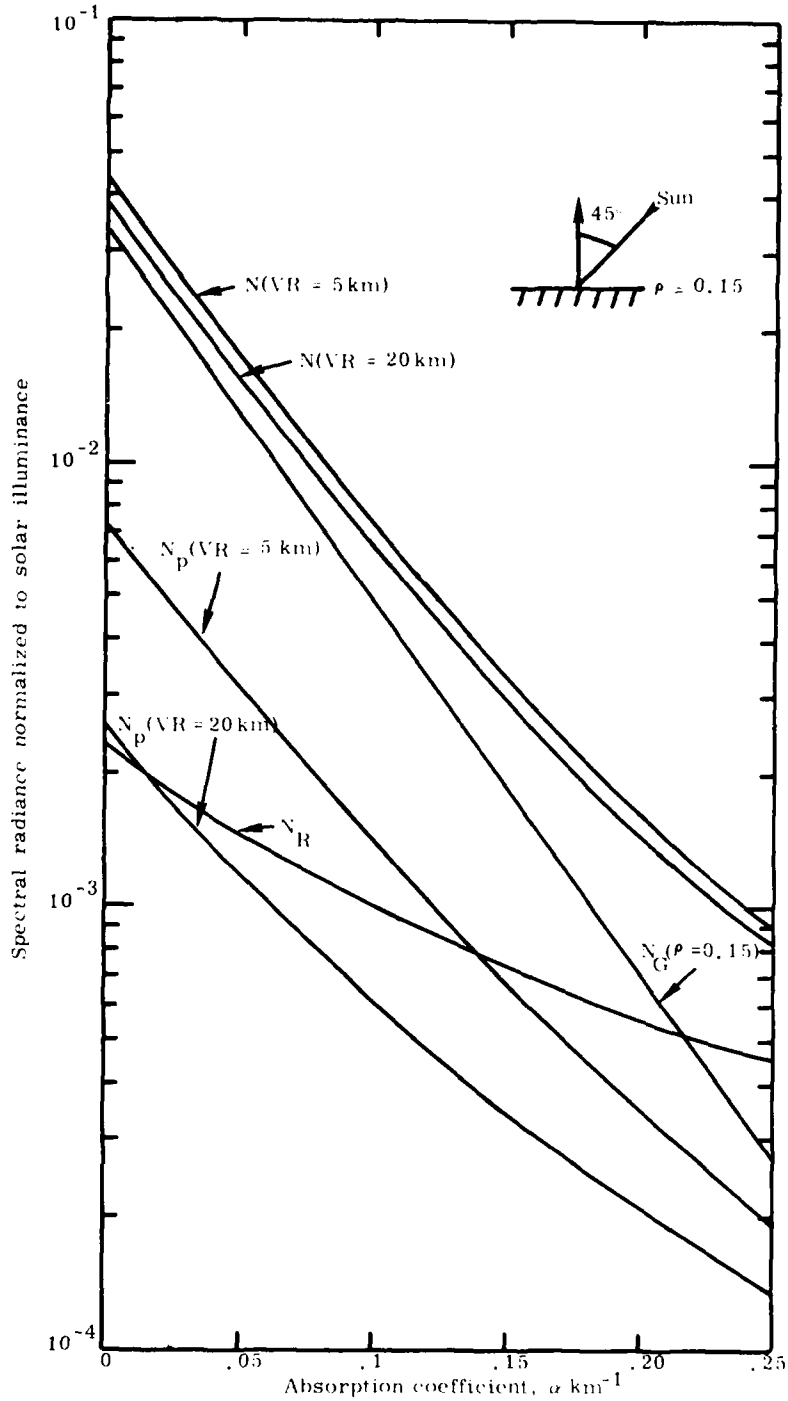

Figure 4.8. Calculated spectral radiance of the atmosphere in different parts of the oxygen A-band (characterized by absorption coefficient α) seen from above for the conditions given on the graph.

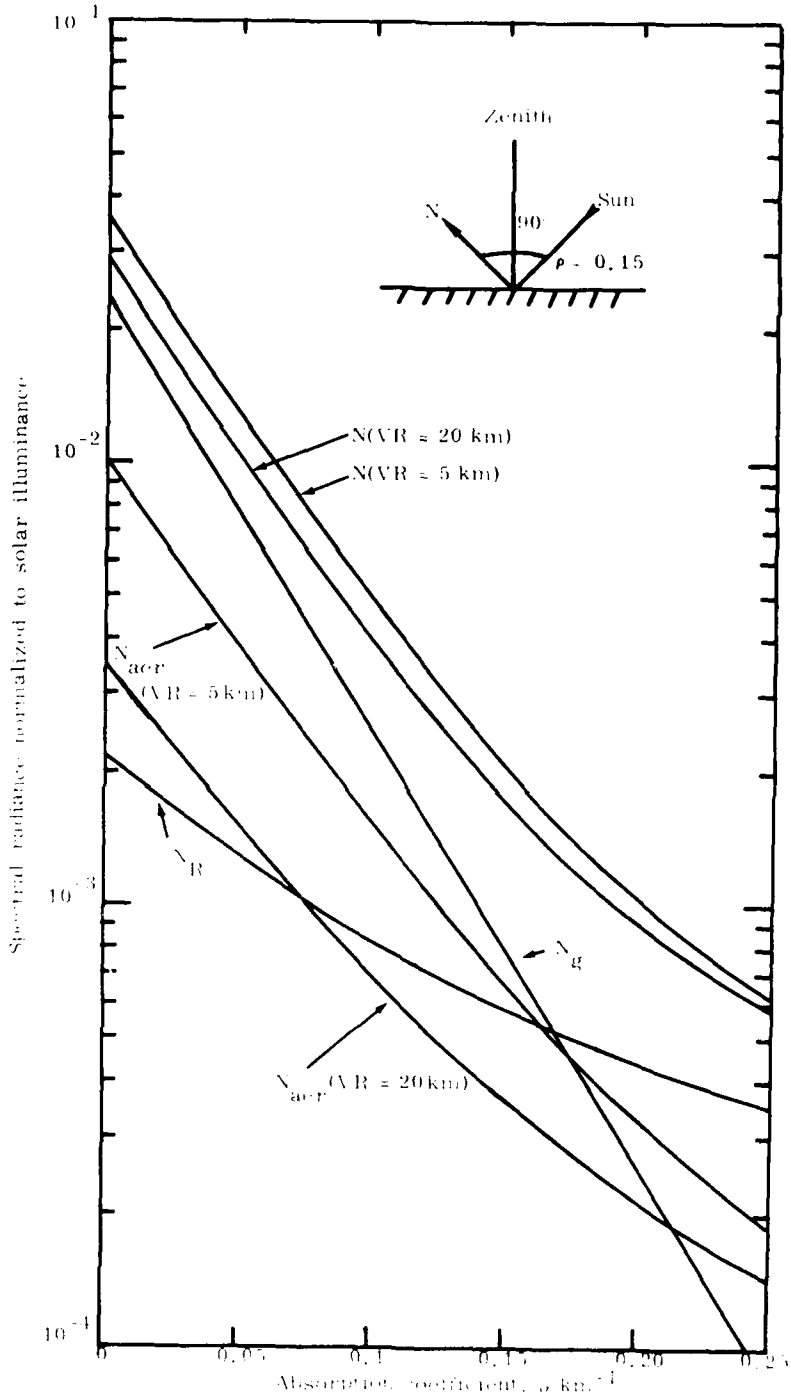

Figure 4.9. Calculated spectral radiance of the atmosphere in different parts of the oxygen A-band (characterized by absorption coefficient σ) seen from above for the conditions given on the graph.

5. ACTIVE REMOTE SENSING

The previous section has described ways of measuring the aerosol content of the lower troposphere using mainly scattered sunlight but also considering the use of light sources on the earth at night. Another possible way of measuring these aerosols is to use active light sources in artificial satellites. The only feasible source is a pulse laser used in a lidar configuration. Both technical and political considerations affect the use of this source. The important technical factors are theoretical feasibility, engineering practicality, and safety. Lidars have been in use for many years for measurement of aerosols along paths near the surface of the earth and for measuring the vertical distributions of aerosols along vertical paths extending to the stratosphere. The theoretical principles of their use have been well established. Two studies of the feasibility of using satellite based lidars to measure the content of aerosols and other constituents in the atmosphere are given in References 31 and 32. While Reference 31 limits its consideration to aerosols above 10 km and does not address our problem, it does provide much informative review and discussion.

Reference 32 presents a detailed discussion of lidar systems which might be useful to measure aerosol distribution from the proposed Space Shuttle. They conclude that an eyesafe system operating from an altitude of 185 km is theoretically possible but that it was at the limit of current technology (1972). The system operates in high spectral resolution (0.002 A) both at the transmitter and receiver. Fabry-Perot etalons are used to obtain this resolution. The source was a N_2 stimulated (3371 A) laser pumping a dye (4000-5000 A) in a laser-etalon-amplifier configuration. The energy per pulse was 50 mJ, the pulse duration was 7 ns, and the repetition rate was 60 Hz.

It is of interest to compare this proposed system with the system that is currently being suggested for Space Shuttle use (Reference 33). Table 5.1 taken from this reference summarizes parameters needed to trace global flow of pollutants including aerosols. There are to be other measurements of other parameters related to meteorology, chemical composition, transport of thermospheric atomic species and others. A standard hardware set to be used for all experiments is given in Table 5.2. Finally, the outline of the experiment is given in Table 5.3. It will be of great interest to follow the progress of these proposed active remote-sensing experiments.

Table 5.1. Parameter Summary Extracted from Reference 33

SUMMARY OF PARAMETERS TO BE MEASURED TO TRACE GLOBAL FLOW OF POLLUTANTS

Parameter	Height Range	Δx	Δx	Remarks	Exp. No.
Aerosols	0-10	100	1	20%, haze layers, thin cirrus, Saharan & Mongolian dust	2, 3
	10-30	500	2	20%, stratospheric aerosols	6, 24
H_2O	0-10	100	1	20 %	9, 10
	10-20	500	2	20 %	
	total	100	**	20 %	
O_3	0-10	100	1	20 %	10, 12 18, 17
	10-30	500	2	20 %	
XY: e.g., SO_2	0-10	100	1	20 %	10, 18, 23
GH_4 NH_3, NO_2, N_2O, CFMs, etc.	10-50	500	3	20 %	
	total	100	**	20 %	
Temperature	0-3	100	0.2	1K, Define boundary layer	17
	5-20	500	1	2K, Define tropopause	
V_x	0-10	100	1	5 m/s	19, 20
	10-50	500	2	10 m/s	
V_z	0-10	100	1	5 cm/s	
	10-50	500	2	10 cm/s	
CO_2 mixing ratio	0-3	100	3	1%, Identify sources and sinks	

Table 5.2. Lidar System Parameters Extracted from Reference 33

ASSUMED STANDARD HARDWARE SET FOR EXPERIMENT DESCRIPTIONS

Lasers:	
Nd-YAG	1 J/pulse; 10 pps, TEM 00 mode; 15 nsec pulse; $<$ 1 Å linewidth; 5% amplitude stability
Derivatives	X2 - 35 %; X4 - 10 % 600 nm (dye) - 10% (0.05 Å) or 30% (1A) 300 nm (dye X2) - 1% (0.05 Å) or 3% (1A)
CO_2	1 J/pulse; 300 pps; TEM 00 mode; 100 nsec pulse; 10 MHz stability and linewidth in 9-12 μm range on selected lines; continuous tuming and other lines available at 10-30%
Derivatives	X2 - 20 $\longrightarrow$ 30% using Cd G-As_2 for 4.5 - 6.2 μm
Receiver Telescope:	1 meter diameter, 0.2 - 12 μm range

Table 5.3. Aerosol Profiling Experiment Extracted from Reference 33

PROFILING OF TROPOSPHERIC CLOUDS AND AEROSOLS

Description: Measure the presence, geometrical profiles and backscattering of thin clouds and aerosols - including data on their optical thickness. Co-aligned Earth radiation budget sensor would measure flux and albedo changes; co-aligned passive temperature and humidity sensors would allow assessment of cloud and aerosol effects on passive profilers. Data would document the locations and extent of aerosols and clouds and permit correlation with radiation changes detected by passive sensors. This information is essential for accurate radiation transfer models. The existence of pollution and dust clouds (e.g., Sahara dust) over large areas could be monitored and mapped.

Implementation: Standard Nd-YAG lidar (1X, 2X) with 1 mr FOV, 2 PMT detectors (20 percent QE at 530 nm; 2 percent QE at 1060 nm). Night or day operation. Data system capable of generating spatial profile of return with height resolution of about 150 m. Some simulations are available and sample results are shown in figure (lidar at 180 km, 0.1 J, Rayleigh atmosphere only) for expected single-shot errors. Simulations under development to include tropospheric aerosols, higher laser energy and multi-shot averaging show greatly improved signal to noise. System will be limited by signal levels for very low density aerosols and clouds, and signal measurement errors will be limiting factor. Achieving ±20 percent accuracy in conversion to optical thickness will be difficult a priori but will be aided by 2 backscattering measurements. Even poorer accuracy will be very useful in most applications.

Feasibility: 1A (530 nm), 1B (1060 nm). Experiment design information is available, and a moderate amount of ground-based field data is available in the visible region of the spectrum. The requirement for good range resolution at very low signal levels increases the difficulty.

Needed Developments: Optimization of the 1060 nm system is required and additional simulations of particular cases are needed.

Discussion: At present no other system exists for measuring the spatial distribution of subvisual tropospheric clouds and aerosols. Such data are vital for a more quantitative understanding of the radiation budget and of the operation of currently used passive sensors. In addition, monitoring the motions of the aerosols and clouds provides the means for studying the transport and mixing processes.

6. CONCLUSIONS AND RECOMMENDATIONS

This review set out to answer the question of whether there existed in the published literature any methods for remote sensing atmospheric visibility. Our studies have led us to the conclusion that although there exist several promising techniques of remotely monitoring atmospheric visibility there is no proven technique which can be immediately put to use. In fact only two or three methods have actually been subjected to testing using real satellite observations. Also it should be recalled that these methods do not monitor visibility itself but rather the total optical transmission of the atmosphere. A separate calculation must be performed to determine visibility for the actual optical system and environmental situation under consideration. More specifically, the three concepts which have been subjected to some degree of experimental verification are:

1. *Contrast Reduction* (See Section 4.1).
2. Upwelling spectral radiance (See Sections 4.2 and 4.3).
3. Angle-integrated Radiance Difference (See Section 4.4).

However, more experimental measurements will be needed to confirm these tentative conclusions and to establish the sensitivity and range of applicability of the method. An important adjunct to these measurements is accurate measurement of the ground-truth values used for comparison. Because of the variability of atmospheric conditions, these measurements should be carried out in a continuous series extending for a minimum of 2 to 3 months.

In the course of this review, a new concept for measuring the optical depth of the atmosphere was developed that makes use of nighttime observation of natural or artificial illumination sources on the earth (See Section 4.6). Further theoretical and numerical calculations should be performed to test the possibilities of this technique. If its capabilities pass these additional tests, consideration should be given to verifying this method using existing observing satellites.

Finally, we make the conjecture that any operational system would depend not on a single method but would be a composite of several techniques mutually supporting and checking the others. To this end, we believe that as many as possible of the candidate methods should be carried forward through the various development stages.

REFERENCES

1. R.S. Fraser, "Computed Atmospheric Corrections for Satellite Data", in Proc. of the Soc. of Photo-Opt. Instr. Eng. Vol. 51, 64-72, Scanners and Imagery Systems for Earth Observation (1974).

2. S. F. Singer & R. C. Wentworth, "A Method for the Determination of the Vertical Ozone Distribution from a Satellite", J. Geophy. Res. 62 300-308, (1957).

3. J. T. Houghton & F. W. Taylor, "Remote Sounding from Artificial Satellites and Space Probes of the Atmospheres of the Earth and the Planets", Rep. Prog. Phys 36, 827-919 (1973).

4. George C. Sherman, "Satellite Based Remote Probing of Atmospheric Visibility: A Bibliography of Relevant Literature", 1976 USAF-ASEE Summer Faculty Research Program, Participants Final Report; 3 Sept. 1976.

5. G. V. Rozenburg & A. B. Sandomierskii, "Determination of Altitude Variations of the Scattering Coefficient from Photographs of Earth's *Day Horizon Obtained from Spaceship* "Voskhod", *Atmospheric* and Oceanic Physics 3, 86-93 (1972).

6. M. P. McCormick et al, "Satellite Studies of the Stratospheric Aerosol", Bull. Am. Met. Soc. 60 1038-46 (1979).

7. Earl J. McCartney, Optics of the Atmosphere, John Wiley and Sons, New York (1976).

8. W. E. K. Middleton, Vision Through the Atmosphere, Univ. of Toronto Press (1952).

9 Douglas V. Hoyt, "A Redetermination of the Rayleigh Optical Dept. and Its Application to Selected Solar Radiation Problems", J. of Appl. Meteor. 16, 432-36 (1977).

10. D. Deirmendjian, Electromagnetic Scattering on Spherical Polydispersions, American Elsevier Publishing Co., Inc (1969).

11. Eric P. Shettle & Robert W. Fenn, "Models of the Atmospheric Aerosols and their Optical Properties", in Optical Propagation in the Atmosphere, AGARD Conf. Proc. No. 183 (Available from NTIS-Accession No. AD-A028-615).

12. Louis Elterman, "Vertical-Attenuation Model with Eight Surface Meteorological Ranges 2 to 13 Kilometers", Reprt No. AFCRL-70-0200, March 1970, Air Force Cambridge Research Laboratories.

13. S. Chandrasekhar, Radiative Transfer, Clarendon Press, Oxford (1950); Dover Publications, Inc., New York (1960).

14. V. V. Sobolev, A Treatise on Radiative Transfer, Van Nostrand Company, Inc., Princeton, N.J., 1963.

15. Gilbert N. Plass & George W. Kattawar, "Calculations of Reflected and Transmitted Radiance for Earth's Atmosphere", Appl. Optics, 7, 1129-35 (1968).

16. James E. Hansen & Larry D. Travis, "Light Scattering in Planetary Atmospheres", Space Sci. Rev. 16, 527-610 (1974).

17. William Irvine, "Multiple Scattering in Planetary Atmospheres", Icarus 25, 175-204 (1975).

18. Jacqueline Lenoble (ed.), Standard Procedures to Compute Atmospheric Radiative Transfer in a Scattering Atmosphere, International Assoc. of Meteorology and Atmospheric Physics (IAMAP) Radiation Commission, July 1977, National Center for Atmospheric Research, Boulder, Colorado.

19. S. Q. Duntley, "The Reduction of Apparent Contrast by the Atmosphere", J. Opt. Soc. Am. 38, 179-91 (1948).

20. Michael Griggs, "Determination of Aerosol Content in the Atmosphere", in Symposium on Significant Results Obtained from the Earth Resources Technology Satellite-1, Vol 1: Technical Presentations Section B, Paper 12, NASA SP-327, National Aeronautics and Space Administration, 1973.

21. A. P. O' Dell & J. A. Weinman, "The Effect of Atmospheric Haze on Images of the Earth's Surface", J. of Geoph. Res. 80, 5035-40 (1975).

22. Michael Griggs, "Measurements of Atmospheric Aerosol Optical Thickness over Water Using ERTS-1 Data", J. of the Air Poll. Contr. Assoc. 25 622-26 (1975).

23. _____ "Comments on 'Relative Atmospheric Aerosol Content from ERTS Observations'", J. Geophys. Res. 82, 4972 (1977).

24. _____ "Satellite Observations of Atmospheric Aerosols during the EOMET Cruise", pp 291-301 in The EOMET Cruise of the USNS Hayes: May-June 1977, Stuart G. Gathman and Ben G. Julian, eds., NRL Memorandum Report 3924, 31 Jan 1979.

25. Yu. Mekler, H. Quenzel, G. Ohring, & I. Marcus, "Relative Atmospheric Aerosol Content from ERTS Observations", J. Geophys. Res. 82, 967-70, (1977).

26. P. Koepke & H. Quenzel, "Remote Sensing of Atmospheric Turbidity from GeoSynchronous Orbit", Paper Tu B3 in Atmospheric Aerosols: Their Optical Properties and Effects, NASA CP-2004, National Aeronautics and Space Administration, 1976.

27. F. J. Ahearn, D. G. Goodenough, S. C. Jain, V. R. Rao, & G. Rochon, "Use of Clear Lakes as Standard Reflectors for Atmospheric Measurements", in Proc. 11th Intern Symp. on Remote Sensing of Environment Vol 1, p 731-55 (1977).

28. G. Sh. Livshits, V. I. Syachinov & E. L. Teen, "Determination of the Optical Thickness of the Atmosphere from Satellites", Atmospheric and Oceanic Physics 9, 169-70 (1973).

29. Owen K. Garriott, "Visual Observations from Space", J. Opt. Soc. Am. 69, 1064-68 (1979).

30. Thomas A. Croft, "Nighttime Images of the Earth from Space", Sci. Am. 239, 86-98 (July 1978).

31. M. L. Wright, E. K. Proctor, L. S. Gasiorek, & E. M. Liston, "A Preliminary Study of Air-Pollution Measurement by Active Remote-Sensing Techniques", NASA CR-132724, National Aeronautics and Space Administration, Hampton, VA. (June 1975).

32. S. T. Shipley, et al, "The Evaluation of a Shuttle Borne Lidar Experiment to Measure the Global Distribution of Aerosols and their Effect on the Atmospheric Heat Budget", Final Report on NASA Grant NSA1057, April 1975, Dept. of Meteorology, University of Wisconsin, Madison, Wisconsin.

33. Robert K. Seals, Jr. & James F. Kilsler (eds.), "Shuttle Atmospheric Lidar Multiple-user Instrument System", National Aeronautics and Space Administration, Langley Research Center, Hampton, VA (no date).

34. V. V. Badayev and M. S. Malkevich, "On the Possibility of Determining the Vertical Profiles of Aerosol Attenuation Using Satellite Measurements of Reflected Radiation in the 0.76 micrometer Oxygen Band", Izvestiya, Atmospheric and Oceanic Physics 14 722-27 (No. 10, 1978).

APPENDIX A

Derivation of Working Equation for Simulated Polar Nephelometer Method of Section 4.4

Figure A1 shows the sun at zenith angle θ_s illuminating the atmosphere. The radiance of the atmosphere is observed at two directions symmetrically located about the zenith at the same angle. The differential equation (DE) governing the transport of radiation along the observation path considering only single scattering is

$$\frac{d B_{1i}}{d s} = -(\beta_{aer} + \beta_R) B_{1i} + (\beta_{aer} \Phi_{aer\,1} + \beta_R \Phi_{R\,1}) H_o e^{-\int_{s'}^{\infty} (\beta_{aer} + \beta_R) d s'} + B_{G1} e^{-\int_o^s (\beta_{aer} + \beta_R) ds} \qquad (A.1)$$

The meaning of the symbols is as follows:

B_{1i} = radiance at position s along path 1 at angle θ_1 to zenith, w cm^{-2} sr^{-1}

s = distance along path 1 measured from origin at surface, km

β_{aer} = scattering coefficient for aerosol, km^{-1}

β_R = Rayleigh scattering coefficient for air molecules, km^{-1}

$\Phi_{aer\,1}$ = scattering phase function for aerosol evaluated for scattering into direction 1

$\Phi_{R\,1}$ = Rayleigh scattering phase function for air molecules evaluated for scattering into direction 1

s' = distance along path to sun measured from origin at surface, km

B_{G1} = radiance of ground surface in direction of path 1, w cm^{-2} sr^{-1}

H_o = irradiance of sun at top of atmosphere, w cm^{-2}

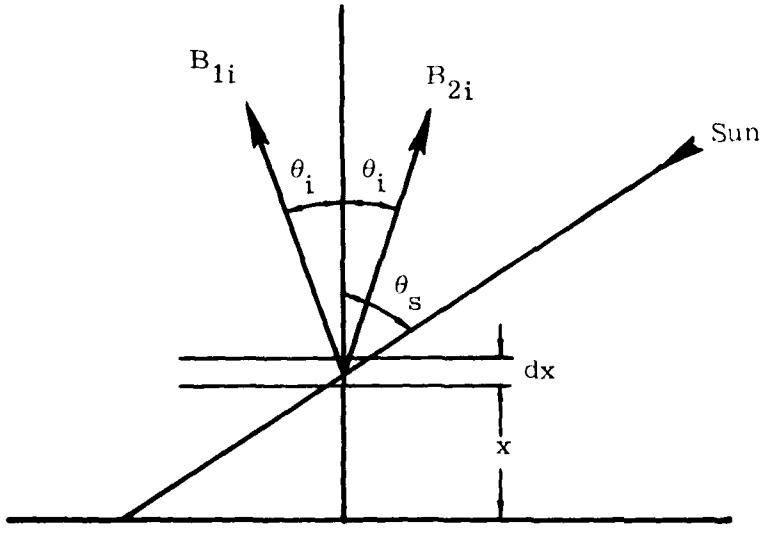

Figure A1. Schematic diagram used to derive working equation for simulated polar nephelometer method.

The differential path elements ds and ds' can be related to the differential element of distance in the zenith direction dx as follows

$$ds = \sec\theta_i\, dx = m_i dx \quad , \quad ds' = \sec\theta_s\, dx = m_s dx \tag{A.2}$$

where the approximate equality between the secant of the zenith angle and atmosphere mass m in the direction having that angle has been used. Assuming that aerosol absorption is small, the optical depth of the atmosphere in the vertical direction can be approximated as

$$\int_o^x (\beta_{aer} + \beta_R)\, dx = \tau_{aer}(x) + \tau_R(x) = \tau(x) \tag{A.3}$$

with $$\int_o^\infty (\beta_{aer} + \beta_R)\, dx = \tau_{o\,aer} + \tau_{oR} = \tau_o \tag{A.4}$$

for the entire atmosphere. Also the differential optical depth is

$$d\tau = (\beta_{aer} + \beta_R)\, dx$$

Now the DE for path 1 can be rewritten as

$$\frac{dB_{1i}}{dx} = -m_i(\beta_{aer} + \beta_R)B_{1i} + m_i(\beta_{aer}\Phi_{aer1} + \beta_R\Phi_{R1})H_o e^{-m_s(\tau_o - \tau(x))} + m_i B_{G1} e^{-m_i \tau(x)} \tag{A.1'}$$

A similar equation for path 2 follows immediately.

Subtracting the two equations leads to a DE for the difference in radiance observed in the two directions 1 and 2.

$$\frac{d\,\Delta B_{12}}{dx} = -m_i(\beta_{aer}+\beta_R)\Delta B_{12} + m_i(\beta_{aer}\Delta\Phi_{aer12}+\beta_R\Delta\Phi_{R12})H_o e^{-m_s(\tau_o-\tau(x))} + m_i\Delta B_{G12}e^{-m_i\tau(x)} \qquad (A.5)$$

Now the last term on the r.h.s. is made to vanish by invoking the assumption that the ground radiance is symmetrical about the zenith angle. The factor in parenthesis in the second term on the r.h.s. is rewritten as follows:

$$(\beta_{aer}\Delta\Phi_{aer\,12}+\beta_R\Delta\Phi_{R12}) = (\beta_{aer}+\beta_R)\Delta\Phi_{aer\,12} + \beta_R(\Delta\Phi_{R12}-\Delta\Phi_{aer\,12}) \qquad (A.6)$$

Thus, the DE in ΔB_{12} is

$$\frac{d}{dx}\Delta B_{12} + m_i(\beta_{aer}+\beta_R)\Delta B_{12} = [m_i(\beta_{aer}+\beta_R)\Delta\Phi_{aer12}+m_i(\beta_R\Delta\Phi_{R12}-\Delta\Phi_{aer12}]H_o e^{-m_s(\tau_o-\tau(x))} \qquad (A.7)$$

Then after dividing through by $(\beta_{aer}+\beta_R)$ and transforming to the optical depth as the independent variable, the DE becomes

$$\frac{d}{d\tau}\Delta B_{12} + m_i\Delta B_{12} = m_i\left\{[\Delta\Phi_{aer12}+\frac{\beta_R}{\beta_R+\beta_{aer}}(\Delta\Phi_{R12}-\Delta\Phi_{aer12})]\cdot H_o e^{-m_s\tau_o}\right\}e^{m_s\tau} \qquad (A.8)$$

This DE can only be integrated analytically if the term in the square brackets

on the r.h.s. is independent of the optical depth. This is equivalent to assuming both that the ratio $\beta_R/(\beta_{aer} + \beta_R)$ and the phase functions are independent of optical depth. Under these assumptions, the DE becomes

$$\frac{d}{d\tau} \Delta B_{12} + m_i \Delta B_{12} = m_i K e^{m_s \tau} \tag{A.9}$$

The first order linear DE equation is readily solved using Laplace transforms with p as the transform variable and the caret identifying the transformed function.

$$(p + m_i) \hat{\Delta B}_{12} = \frac{m_i K}{p - m_s} + \Delta B_{12} \Big|_{\tau = o} \tag{A.10}$$

Since $\Delta B_{12} \Big|_{\tau = o} = o$, the equation is

$$\hat{\Delta B}_{12} = \frac{m_i K}{(p + m_i)(p - m_s)} \tag{A.11}$$

Applying the inverse transform, the difference in radiance is

$$\Delta B_{12}(\tau) = \frac{m_i}{m_i + m_s} K (e^{m_s \tau} - e^{-m_i \tau}) \tag{A.12}$$

$$= \frac{m_i H_o}{m_i + m_s} \left\{ \left[\Delta\Phi_{aer12} + \frac{\beta_R}{\beta_{aer} + \beta_R} (\Delta\Phi_{R12} - \Delta\Phi_{aer12}) \right] e^{-m_s \tau_o} \right\} (e^{m_s \tau} - e^{-m_i \tau})$$

$$= \frac{m_i H_o}{m_i + m_s} \left[\Delta\Phi_{aer12} + \frac{\beta_R}{\beta_{aer} + \beta_R} (\Delta\Phi_{R12} - \Delta\Phi_{aer12}) \right] \cdot$$

$$(e^{-m_s(\tau_o - \tau)} - e^{-m_s \tau_o - m_i \tau})$$

When evaluated at $\tau = \tau_o$ i.e. from outside the atmosphere, the expression

becomes

$$\Delta B_{12}(\tau_o) = \frac{m_i H_o}{m_i + m_s} \left[\Delta\Phi_{aer12} + \frac{\beta_R}{\beta_{aer} + \beta_R} (\Delta\Phi_{R12} - \Delta\Phi_{aer12}) \right] \cdot \left(1 - e^{-(m_i + m_s)\tau_o} \right) \quad \text{(A.13)}$$

Now make the following algebraic manipulations.

$$\Delta\Phi_{aer12} + \frac{\beta_R}{\beta_{aer} + \beta_R} (\Delta\Phi_{R12} - \Delta\Phi_{aer12}) = \frac{\Delta B_{12}(\tau_o)(m_i + m_s)}{H_o m_i (1 - e^{-(m_i + m_s)\tau_o})} \quad \text{(A.14)}$$

$$(\beta_{aer} + \beta_R)\Delta\Phi_{aer12} + \beta_R(\Delta\Phi_{R12} - \Delta\Phi_{aer12}) = \frac{\Delta B_{12}(m_i + m_s)(\beta_{aer} + \beta_R)}{H_o m_i (1 - e^{-(m_i + m_s)\tau_o})} \quad \text{(A.15)}$$

If the phase functions $\Phi_{aer\,12}$ and Φ_{R12} are independent of altitude, an integrationover the height of the atmosphere can be done and it produces

$$\tau_{o\,aer}\Delta\Phi_{aer12} + \tau_{oR}\Delta\Phi_{R12} = \frac{\Delta B_{12}(m_i + m_s)(\tau_{o\,aer} + \tau_{oR})}{H_o m_i (1 - e^{-(m_i + m_s)\tau_o})} \quad \text{(A.16)}$$

The Rayleigh phase function is always independent of altitude (neglecting depolarization). For the aerosol phase function to be independent of altitude requires that the size distribution and composition be independent of altitude which in general is not true. However, in the boundary layer which contains most of the optical thickness of the atmosphere, this condition of altitude independence is approximately true.

The final step is to integrate both sides of Eq. (A.16) over the scattering angle. To arrive at the correct expression for the optical depth of the atmosphere, it must be assumed that the integral over the phase function in the back scattering region can be neglected compared to the forward scattering contribution. The consequence is that the method cannot be absolute but a correction or calibration factor must be obtained from a separate experiment.

The formal solution which results after integrating over all scattering angles and using the above assumption is

$$\tau_{o\,aer}\, 2\pi \int_o^{\pi} \Phi_{aer\,1} \sin\theta \, d\theta = \tau_{o\,aer} \tag{A.17}$$

$$= 2\pi \int_o^{\pi} d\theta \sin\theta \left\{ \frac{\Delta B_{12} (\tau_{o\,aer} + \tau_{o\,R})(m_i + m_s)}{H_o m_i (1 - e^{-(m_i + m_s)\tau_o})} - \tau_R \Delta\Phi_{R12} \right\}$$

which is the working equation for this method. The analogous working equation for the ground based method is

$$\tau_{o\,aer} = 2\pi \int_o^{\pi} d\theta \sin\theta \left\{ \frac{\Delta B_{12} (\tau_{o\,aer} + \tau_{o\,R})(m_i - m_s)}{H_o m_i (e^{-\tau_o m_s} - e^{-\tau_o m_i})} - \tau_R \Delta\Phi_{R12} \right\} \tag{A.18}$$

APPENDIX B

Solution of Transcendental Equation for τ_o and d

In Section 4.5, a method is given for obtaining the vertical optical thickness from measurements of the angular variation of the nighttime intensity of a city. The unattenuated intensity will have a complex angular variation which is unknown. The analysis of Section 4.5 assumed that the variation had only a constant term and a cosine term with the relative contribution of the two unknown. A single transcendental equation relating the vertical optical thickness τ_o and a term d which gives the proportion of the cosine variation was derived. This appendix gives a numerical method for solving this equation when measurements are given.

The basic equation is

$$j(\tau_o, w) = \left[1 - d \left(\frac{w}{w+1} \right) \right] e^{-\tau_o w} \tag{B.1}$$

where $w = \sec\theta - 1$ and $w/(w+1) = 1 - \cos\theta$.

An easy algebraic manipulation gives

$$e^{\tau_o} = \left\{ \frac{1}{j} \left[1 - d \left(\frac{w}{w+1} \right) \right] \right\}^{\frac{1}{w}} \tag{B.2}$$

and

$$\tau_o = \frac{1}{w} \ln \left\{ \frac{1}{j} \left[1 - d \left(\frac{w}{w+1} \right) \right] \right\} \tag{B.3}$$

It is also easy to solve for d, i.e.

$$d = \frac{w+1}{w} \left[1 - j e^{\tau_c w} \right] \tag{B.4}$$

Now write down the two equations for τ_o using two measurements j_1 and j_2.

$$\tau_o = \frac{1}{w_1} \ln \left\{ \frac{1}{j_1} \left[1 - d \left(\frac{w_1}{w_1 + 1} \right) \right] \right\} \qquad (B.5)$$

$$\tau_o = \frac{1}{w_2} \ln \left\{ \frac{1}{j_2} \left[1 - d \left(\frac{w_2}{w_2 + 1} \right) \right] \right\} \qquad (B.6)$$

Figure B1 shows that when plotted as a function of d, these two curves intersect and give a common solution for τ_o and d.

To find the numberical values at the intersection, rewrite one of the equations in the form giving d explicitly , say

$$d = \frac{w_2 + 1}{w_2} \left[1 - j_2 e^{\tau_o w_2} \right] \qquad (B.7)$$

Make an initial estimate of where the solution is located. Insert the value of d into the equation for τ_o. Use the value to obtain a new value of d.

Continuation of these steps produces a sequence of values of τ_o and d which converge to the desired solution. A geometric diagram of the process is given in Figure B2. For the process to converge, the sequence must be to find τ_o from function 1 and d from function 2. Convergence is obtained regardless of whether the initial value is greater than or less than the solution. If the roles of 1 and 2 were reversed in this example, the sequence of values would diverge. One concludes that convergence depends on the relative slopes of the two curves. Thus if divergence occurs, a reversal of the equation should induce convergence.

This process is readily carried out with a small programmable calculator. All of the results given in Section 4.5 were obtained with a Hewlett-Packard HP-55 calculator. Table B1 shows the rapid convergent sequence for an example where the correct solution is $\tau_o = 0.1$ and $d = 0.2$. Values of j_1 and j_2 correct to 4 decimal places are used. Two initial values for d are tried, 0 and 1, which are the extremes of that variable.

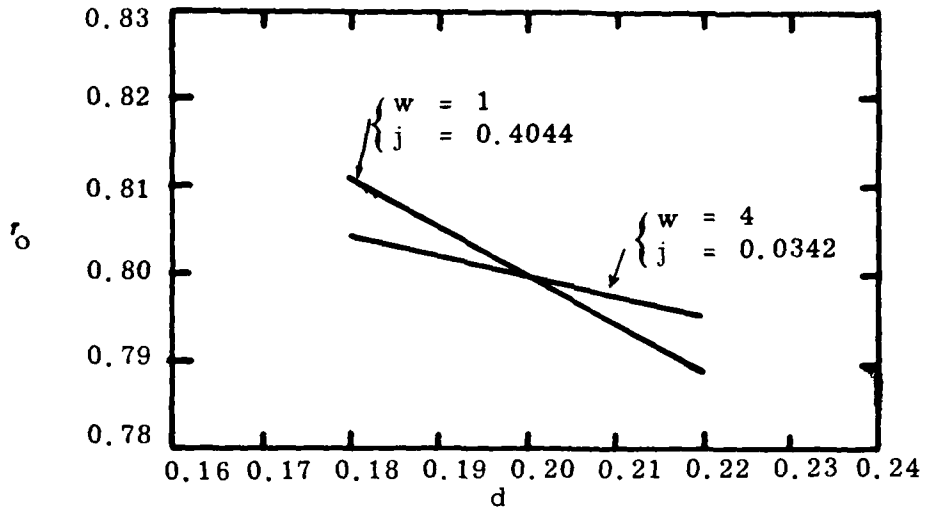

Figure B1. Plot of Equations B5 and B6 showing intersection solution.

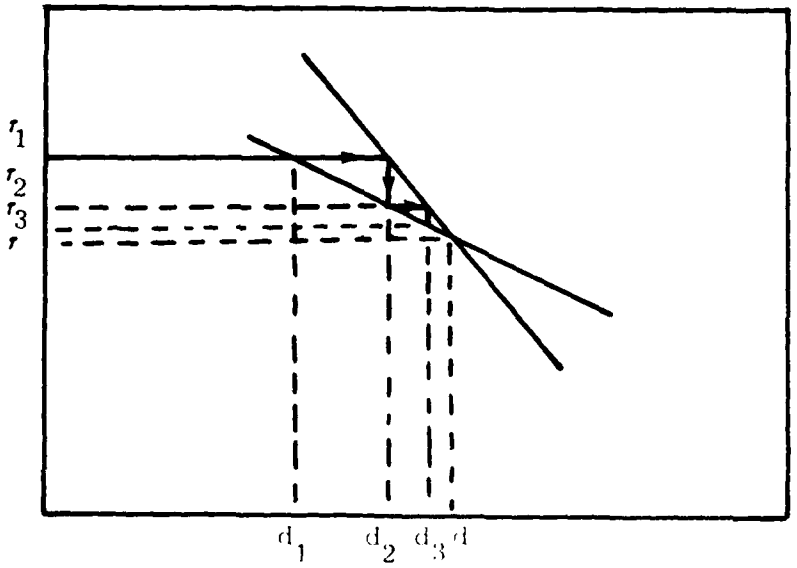

Figure B2. Schematic diagram of iterative solution of Equations B5 and B7.

Table B1. Examples of Converging Sequence Values in the Solution of the Transcendental Equation for τ_o and d.

CASE A		CASE B	
d	τ_o	d	τ_o
0.00000	.11054	1.00000	-.11973
.18792	.10133	.44951	.06753
.19861	.10015	.23770	.09572
.19998	.10000	.20512	.09943
.20016	.09998	.20082	.09991
.20018	.09998	.20026	.09997
		.20019	.09998
		.20018	.09998

APPENDIX C

First Order Downward Scattering of Sunlight

We consider sunlight incident on a clear atmosphere from any zenith angle and ask the question--for those photons which are scattered in the atmosphere before reaching the ground, what is the probability that the first scattering event will direct the photon in a downward direction?

Here we will answer the question at wavelength $\lambda = 0.45\mu$ simply because we have the necessary tools at hand to do this. Deirmendjian's haze model L (continental haze) is used to represent the scattering characteristics of the aerosols involved. The optical depth of the atmosphere when the zenith angle considered is zero $\tau(o)$ is described here as follows:

$$\tau(o) = \int_o^\infty [\sigma_a(h) + \sigma_m(h)]\, dh = \int_o^\infty \sigma_a(h)\, dh + \int_o^\infty \sigma_m(h)\, dh \qquad (C.1)$$

where $\sigma_a(h)$ is the aerosol scattering coeffieient at altitude h

$\sigma_m(h)$ is the molecular scattering coefficient at altitude h

The contribution of the molecular scattering may be written

$$\int_o^\infty \sigma_m(h)\, dh \approx 8\, \sigma_m(o) = \tau_m(o) \qquad (C.2)$$

and at $\lambda = 0.45\mu$ $\sigma_m = 2.72 \times 10^{-2}$ or $\tau_m(o) = 0.217$. The normalized phase function for molecular scattering of unpolarized light $\Phi(\alpha)$ is given by

$$\Phi(\alpha) = \frac{3}{16\,\pi}(1 + \cos^2\alpha)\ , \ sr^{-1} \qquad (C.3)$$

where α is the scattering induced angle of deviation of the incident ray.

---

* Height of homogeneous atmosphere = 8 km

This implies that the three dimensional distribution of the directional probability of scattering has a center of symmetry. Hence, no matter what the angle of incidence on the atmosphere of light the probability that light scattered by molecules will be deviated into a downward direction is 0.5

This contribution to the optical depth made by the aerosols, τ_a, depends on their concentration. If the optical depth τ is known or assumed then

$$\tau_a(o) = \tau(o) - 0.217 \qquad (C.4)$$

and, more generally, if ϕ is the zenith angle at which the optical depth of the atmosphere $\tau(\phi)$ is evaluated then

$$\tau_a(\phi) = \tau_a(o) \sec \phi = \tau(\phi) - 0.217 \sec \phi \qquad (C.5)$$

Assuming no absorption in the atmosphere, the fraction of the light incident at zenith angle ϕ which is scattered before reaching the ground, s, is given by

$$s = 1 - e^{-\tau(\phi)} \qquad (C.6)$$

The fraction scattered by molecules, s_m is

$$s_m = \frac{\tau_m(\phi)}{\tau(\phi)} = \frac{\tau_m(o)}{\tau(o)} = \frac{0.217}{\tau(o)} \qquad (C.7)$$

The fraction scattered by aerosols, s_a, is

$$s_a = \frac{\tau_a(o)}{\tau(o)} = \frac{\tau(o) - 0.217}{\tau(o)} \qquad (C.8)$$

Figure C1 is a semilog plot of the normalized phase function for aerosol scattering of unpolarized light at wavelength $\lambda = 0.45\mu$. The aerosol considered is Deirmendjian's model L and the solid line is drawn through his values as reported in Reference 10. The following equation has been cooked-up to match the solid curve:

$$\Phi(\alpha) = 10^{+\left\{2.183 \times 10^{-4} (115 - \alpha)^2 - 2.196\right\}} \quad , \alpha \leq 153°$$

$$= 10^{\left\{0.075 \sin \frac{(\alpha - 115)^2}{1.62} - 1.875\right\}} \quad , \alpha > 153° \qquad (C.9)$$

The circled points in Figure C1 were calculated using Equation C9.

Deirmendjian's phase functions are normalized so that

$$2\pi \int_0^{180°} \Phi(\alpha) \sin \alpha \, d\alpha = 1 \qquad (C.10)$$

Using Equation C9 for values of $\Phi(\alpha)$ and approximating the integral by a sum we have calculated with $\Delta\alpha = 2°$

$$\sum_{n=1}^{90} \Phi(2n-1) \sin(2n-1) \Delta\alpha = 0.7885 \qquad (C.11)$$

In what follows a normalizing factor has been introduced to force the sum calculated by Equation C11 to equal unity.

To calculate $R_a(\phi)$, the fraction of the scattered radiation which directed in a downward direction when the solar zenith angle is ϕ, the following equation was written

$$R_a(\phi) = 2\pi \int_0^{180°} \Phi(\alpha) f(\alpha) \sin \alpha \, d\alpha \qquad (C.12)$$

where $f(\alpha)$ is used in the range $0 \leq \alpha \leq 90°$.

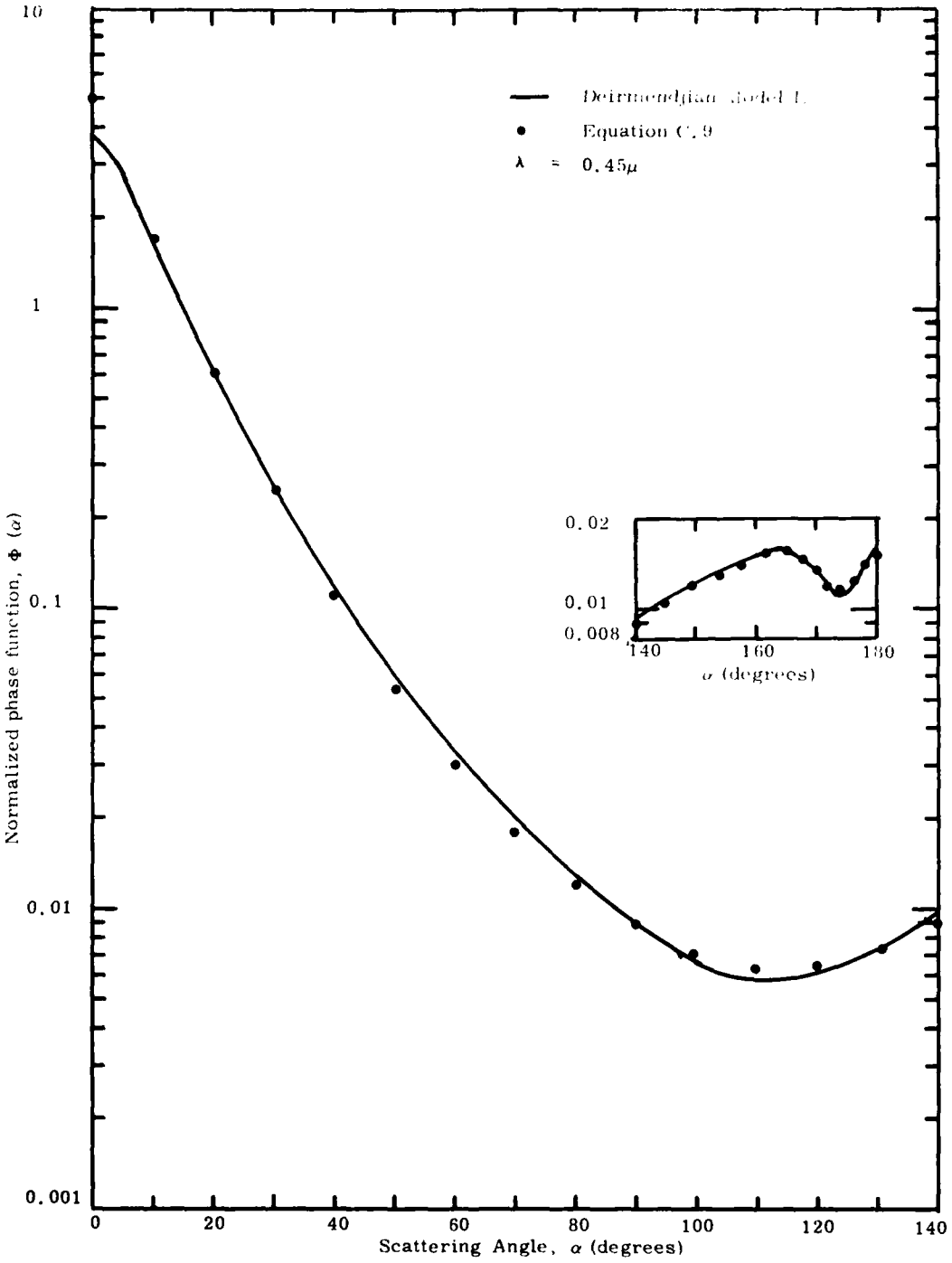

Figure C.1. Normalized phase function for unpolarized light at 0.45 microns as given by Deirmendjian (solid curve) and calculated by fitted Equation C.9 (circled points).

$$f(\alpha) = 1 \qquad \text{for} \quad \frac{90° - \phi}{\alpha} \geq 1$$

$$= \frac{180° - \cos^{-1}\left(\frac{90 - \phi}{\alpha}\right)}{180°} \quad \text{for} \quad \frac{90° - \phi}{\alpha} < 1$$

and where $f(\alpha)$ is used in the range $90° < \alpha \leq 180°$

$$f(\alpha) = 0 \qquad \text{for} \quad \frac{90° - \phi}{180° - \alpha} \geq 1$$

$$\text{and } f(\alpha) = \frac{\cos^{-1}\left(\frac{90° - \phi}{180° - \alpha}\right)}{180°} \quad \text{for} \quad \frac{90° - \phi}{180° - \alpha} < 1$$

The summing approximation illustrated by Equation C11 was used to obtain values of $R_a(\phi)$ from Equation C12. Values calculated are presented in column 1 of Table C1 and are plotted in Figure C2.

The second column of Table C1 gives the fraction of molecular scattered light directed in a downward direction. The third and fourth columns give this fraction for two values of the vertical optical depth of the atmosphere. Equations C7 and C8 were used to calculate the fraction of the total scattering due to aerosols and due to molecules.

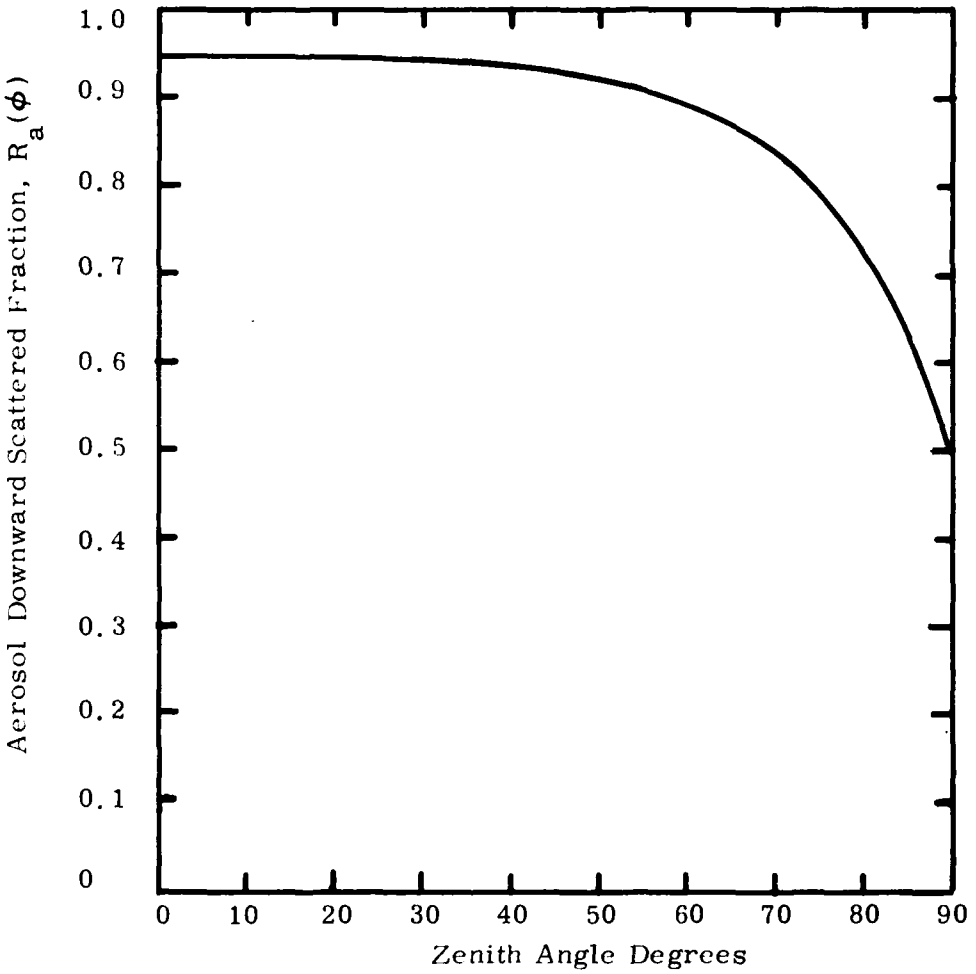

Figure C.2. First order downward scattered fraction of light scattered at 0.45 microns by Model I aerosols.

TABLE C1

Zenith Angle	Aerosol Downward Fraction	Molecular Downward Fraction	R (o)	
			$\tau = 0.6$ Downward Fraction	$\tau = 0.4$ Downward Fraction
0	.947	.50	.785	.705
10	.947	.50	.785	.705
20	.946	.50	.785	.704
30	.943	.50	.783	.703
40	.937	.50	.779	.700
50	.924	.50	.771	.694
60	.898	.50	.754	.682
66	.871	.50	.737	.640
70	.844	.50	.720	.657
76	.785	.50	.682	.630
80	.729	.50	.646	.605
82	.693	.50	.623	.588
84	.658	.50	.601	.572
86	.607	.50	.568	.549
88	.556	.50	.536	.526
90	.500	.50	.500	.500

First Order Downward Scattered Fraction of Scattered Light, $R(\phi)$ at $\lambda = 0.45\mu$ for Haze Model L, for Molecular Scattering and for Two Values of Vertical Optical Depth of the Atmosphere.

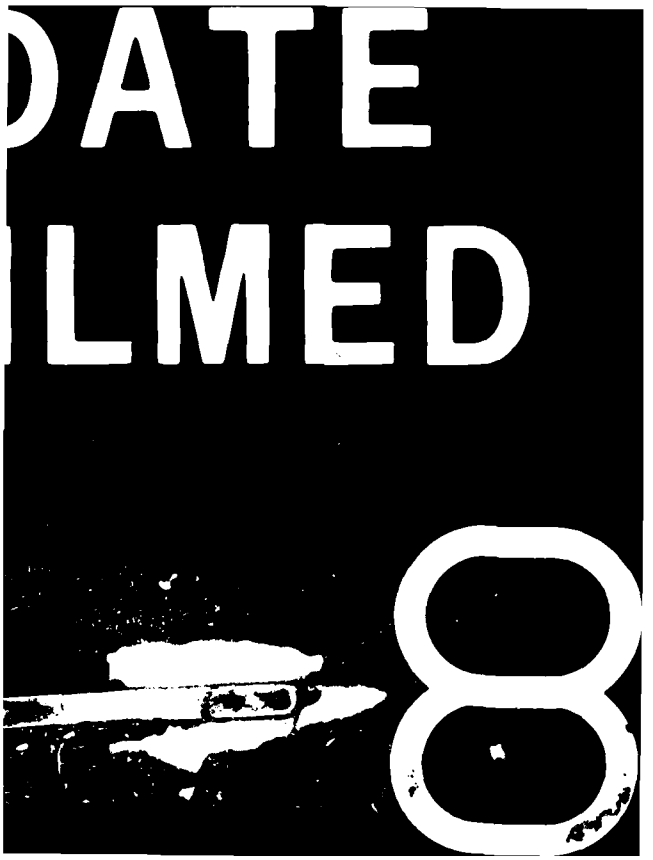
DATE
LMED
8